

If it so happens that $\gamma(\omega)$ is independent of frequency then γ_T will be independent of temperature. Then the solid obeys the Grüneisen's law over the entire temperature range. Such a solid is called a *perfect Grüneisen solid*.

This is as far as the general theory of thermal expansion can go. If we want to make a detailed calculation of the temperature dependence of γ_T for comparison with experiment, we would have to formulate a model for the forces in the crystal. Such detailed calculations have been done for several crystal structures. We could reverse the procedure and analyse the experimentally observed γ_T to obtain values of some of the $\gamma(n)$. This is important because a knowledge of the $\gamma(n)$ allows us to predict the volume dependence of other properties such as the entropy, zero-point energy and the Debye-Waller factors. These aspects will be discussed later.

3.2. CALCULATION OF γ_0 FROM THE PRESSURE DEPENDENCE OF THE SECOND-ORDER ELASTIC CONSTANTS

As mentioned before, the low temperature limit of γ_T , namely γ_0 , depends only on the variation of the elastic frequencies of the lattice with volume. The pressure dependence of the second-order elastic constants of a number of cubic crystals has been studied by Lazarus (626) and others (1157, 1303, 1409). From the pressure dependence of the second-order elastic constants one can obtain the volume dependence of c_{11} , c_{12} and c_{44} , which can then be used to calculate the volume dependence of the elastic wave velocities in any direction in the crystal. This provides the values of $\gamma_j(\theta, \phi)$, $j = 1, 2, 3$, in equation (3.1.17). The $\gamma_j(\theta, \phi)$ is given by

$$\gamma_j(\theta, \phi) = \frac{1}{3} - \frac{\partial \ln s_j(\theta, \phi)}{\partial \ln V} \quad (3.2.1)$$

These values may then be used in equation (3.1.17) to calculate γ_0 . This was done by Sheard (984) for copper, aluminium, sodium and potassium chlorides. Sheard calculated $\gamma_j(\theta, \phi)$ for several directions in reciprocal space and evaluated γ_0 by numerical integration using a computer. Daniels (215, 216) used the tables of De Launay (234, 235, 236) to find the values of γ_0 for Germanium and Silicon from the measured pressure dependence of the elastic constants. If the anisotropy of the integrand in equation (3.1.17) does not exceed certain limits, this is perhaps the easiest way of obtaining γ_0 to a fair degree of accuracy. However, this method has not been used by others. Collins (191) has

used a six-direction Houston's method developed by Betts et al. (94) to find γ_0 for some metals and for NaCl and KCl. The six term Houston's method also yields fairly accurate results without laborious computation as long as the anisotropy of the integrands is not large. Schuele & Smith (958) have worked out a computer programme for calculating γ_0 . The γ_0 values of a number of crystals, for which the pressure dependence of the second-order elastic constants has been measured, have been computed using this programme. There is one point to be borne in mind in comparing such calculations with experiment. What is needed for the calculation of γ_0 is the pressure dependence of the elastic constants at the Absolute Zero. Usually the pressure dependence measured at room temperature is used in these calculations. Also Leibfried & Ludwig (634) have indicated a procedure for finding the c_{ij} 's for the harmonic lattice at the Absolute Zero from a measurement of the temperature dependence of the elastic constants. The authors are not aware of this procedure being ever adopted by any worker in the actual computation of γ_0 .

3.3. ANALYSIS OF EXPERIMENTAL DATA

Fairly accurate measurements of the thermal expansion of a number of crystals down to liquid helium temperatures have been published recently. Together with accurate measurements on the temperature dependence of the specific heat and elastic constants, these measurements provide fairly dependable results on the temperature dependence of the Grüneisen parameter γ_T for these crystals. Barron et al. (68) had previously published a detailed paper on the analysis of the temperature dependence of the specific heat of the alkali halides, and indicated how one could obtain valuable information about the low frequency end of the frequency distribution function and the moment μ_n of the distribution function. Barron et al. (70) have indicated how the temperature dependence of γ_T can be analysed to yield values for $\gamma(n)$. This analysis will be presented in detail here because the observed values of $\gamma(n)$ are important in predicting the volume dependence of other physical properties of the crystal and can be used to test the validity of any model for the anharmonic interactions in a crystal.

(a) Analysis of Specific Heat Data (Barron, Berg & Morrison, 68)

Accurate measurements of specific heat from very low temperatures to moderately high temperatures can be analysed as follows. The measured values of the specific heat are used to get the equivalent Debye temperatures at different values of temperature. This Debye temperature at any

given temperature pertains to the equilibrium volume of the crystal at that temperature. For the quasi-harmonic approximation, these Θ values have to be reduced to the volume of the crystal V_0 at the Absolute Zero of temperature. This is done by scaling the Θ values using the equation

$$\frac{\Theta(V_T)}{\Theta(V_0)} = \left(\frac{\rho_0}{\rho_T} \right)^\gamma \quad (3.3.1)$$

Here ρ_T is the density of the crystal at temperature T , ρ_0 is the density at the Absolute Zero and γ is a constant related to the Grüneisen parameter. Actually the value of γ to be used in the above equation must be a function of temperature; but the average value of γ obtained from measurement of thermal expansion at moderately high temperature was used by these authors. This reduced Debye temperature can be used to find the specific heat of the crystal C_{vhar} in the quasi-harmonic approximation.

At low frequencies the frequency distribution function of any crystal can be expanded in even powers of the frequency, ν

$$G(\omega) = 2\pi G(\nu) = N(\alpha_+ \nu^2 + \beta_+ \nu^4 + \gamma_+ \nu^6 + \dots) \quad (3.3.2)$$

and the specific heat at low temperatures can be correspondingly expanded as

$$C_{vhar} = aT^3 + bT^5 + cT^7 + \dots \quad (3.3.3)$$

The constants α_+ , β_+ , γ_+ are related to a , b , c by the relation

$$\begin{aligned} \alpha_+ &= \frac{15}{8} \frac{a}{\mathcal{D} \pi^4} \left(\frac{h}{k} \right)^3 \\ \beta_+ &= \frac{21}{32} \frac{b}{\mathcal{D} \pi^6} \left(\frac{h}{k} \right)^5 \\ \gamma_+ &= \frac{15}{128} \frac{c}{\mathcal{D} \pi^8} \left(\frac{h}{k} \right)^7 \end{aligned} \quad (3.3.4)$$

where \mathcal{D} is the gas constant. A plot is made of C_{vhar}/T^3 against T^2 . The intercept of this curve on the $T=0$ axis gives the value of a ; and the values of b and c are obtained from the slope and curvature of this curve. The value of a is related to Θ_0 , the low temperature limit of the Debye temperature, which can be calculated from the elastic constants at the Absolute Zero. The accuracy in the determination of a is high; but the accuracy in finding b and c is only moderate. From a , b and c the values of α_+ , β_+ and γ_+ can be found.

In the high temperature limit, C_{vhar} can be expanded in powers of $(1/T)^2$ making use of the Thirring expansion

$$C_{vhar} = 3Nk \left(1 - \frac{\mathcal{B}_2}{21} \frac{\mu_2^*}{T^2} + \frac{3\mathcal{B}_4}{41} \frac{\mu_4^*}{T^4} - \frac{5\mathcal{B}_6}{61} \frac{\mu_6^*}{T^6} + \dots \right) \quad (3.3.5)$$

Here \mathcal{B}_n are the Bernoulli numbers. This expansion converges above a temperature $T \approx 0.2 \Theta_D$. However, the convergence is slow below $T = 0.2 \Theta_D$. Above this temperature anharmonic effects play an important role and it becomes impossible to obtain accurate values of the moments μ_2 and μ_4 making use of this expansion. It is then more profitable to use a high temperature expansion for the reduced Debye temperature Θ_D given by

$$\Theta_D^2 = \Theta_\infty^2 \left\{ 1 - \mathcal{A} \left(\frac{\Theta_\infty}{T} \right)^2 + \mathcal{B} \left(\frac{\Theta_\infty}{T} \right)^4 - \dots \right\} \quad (3.3.6)$$

where

$$\begin{aligned} \Theta_\infty &= \frac{h}{k} \left(\frac{5\mu_2}{3} \right)^{1/2} \\ \mathcal{A} &= \frac{3}{100} \left(\frac{\mu_4}{\mu_2^2} - \frac{25}{21} \right) \\ \mathcal{B} &= \frac{1}{1400} \left(\frac{\mu_6}{\mu_2^3} - \frac{125}{81} - 100\mathcal{A} \right) \end{aligned} \quad (3.3.7)$$

This expansion converges faster than the expansion for C_{vhar} below $T = 0.5 \Theta_D$ and so can be used with advantage in the temperature range $\Theta_D/6 < T < \Theta_D/2.5$ to obtain values of the even moments μ_2, μ_4 and μ_6 . A plot of Θ_D^2 against $1/T^2$ yields a curve whose intercept at $1/T = 0$ gives a value of Θ_∞^2 . Having found Θ_∞ thus, a plot is made of $(\Theta_D^2 - \Theta_\infty^2)/\Theta_\infty^2$ against Θ_∞^2/T^2 . The values of \mathcal{A} and \mathcal{B} are obtained from this plot. Since this function is very sensitive to uncertainties in specific heat values at temperatures greater than $0.5 \Theta_\infty$, the data in the region $\Theta_\infty/2.5 > T > \Theta_\infty/6$ are used to make the extrapolation to $T \rightarrow \infty$. The moments μ_4 and μ_6 can thus be determined. The higher order moments are more inaccurate. The uncertainty in μ_6 in potassium bromide is found to be about 15%.

The other moments can be obtained as follows: the entropy in the harmonic approximation, S_{har} , can be expanded at high temperatures to yield

$$S_{har} = 3Nk \left\{ 1 - \ln \frac{h\nu_g}{kT} + \frac{1}{2} \frac{\mathcal{B}_2}{21} \frac{\mu_2^*}{T^2} - \frac{3}{4} \frac{\mathcal{B}_4}{41} \frac{\mu_4^*}{T^4} + \frac{5}{6} \frac{\mathcal{B}_6}{61} \frac{\mu_6^*}{T^6} - \dots \right\} \quad (3.3.8)$$

The entropy is obtained from the integral

$$S_{har} = \int_0^T \frac{C_{vhar}}{T} \cdot dT \quad (3.3.9)$$

A plot of $\exp[(S - 3Nk)/3Nk]$ against temperature has a slope which yields the value of the geometric mean frequency ν_g .

The zero-point energy is given by

$$\mathcal{E}_Z = \frac{3}{2} N h \nu_1$$

$$= 3NkT \left(1 + \frac{\mathcal{B}_2}{2!} \frac{\mu_2^*}{T^2} - \frac{\mathcal{B}_4}{4!} \frac{\mu_4^*}{T^4} + \frac{\mathcal{B}_6}{6!} \frac{\mu_6^*}{T^6} - \dots \right) - \int_0^T C_{vhar} \cdot dT \quad (3.3.10)$$

from which μ_1 can be determined.

The moments μ_n ($-3 < n < 0$) can be obtained by using Hwang's (482) integral

$$\int_0^\infty \frac{C_{vhar}}{T^n} \cdot dT = 3Nk \Gamma(n+1) \zeta(n) \mu_1^{*-n} \quad (3.3.11)$$

for ($1 < n < 4$).

Here $\Gamma(n+1)$ is the Gamma function and $\zeta(n)$ is the Riemann zeta function. Splitting the integral into two parts

$$\int_0^\infty = \int_0^T + \int_T^\infty$$

and using the expansion for C_{vhar} in the second integral, one gets

$$\begin{aligned} \frac{1}{3Nk} \int_0^T \frac{C_{vhar}}{T^n} \cdot dT &= \Gamma(n+1) \cdot \zeta(n) \cdot \mu_1^{*-n} - \frac{1}{n-1} \frac{1}{T^{n-1}} \\ &+ \sum_{s=1}^\infty (-1)^{s+1} \frac{\mathcal{B}_{2s}}{(2s)!} \frac{2s-1}{(2s+n-1)} \frac{\mu_{2s}^*}{T^{2s+n-1}} \quad (3.3.12) \end{aligned}$$

The temperature T is so chosen that the series on the right converges rapidly.

The above analysis has been used by Barron et al. to find the moments of several alkali halide crystals from the specific heat data.

(b) Analysis of Thermal Expansion Data: (70)

At low temperatures using the expansion for C_{vhar} (3.3.3) and the expression for S_{har} , one finds

$$\gamma_T = \frac{V}{C_{vhar}} \cdot \frac{\partial S_{har}}{\partial V} \Big|_T$$

$$= \left\{ \frac{1}{3} \frac{\partial \ln a}{\partial \ln V} + \frac{b}{a} T^2 \left(\frac{1}{5} \frac{\partial \ln b}{\partial \ln V} - \frac{1}{3} \frac{\partial \ln a}{\partial \ln V} \right) + \dots \right\} \quad (3.3.13)$$

By plotting the values of γ_T against T^2 at low temperatures, a straight line is obtained with an intercept γ_0 equal to the low temperature limit of the Grüneisen parameter. The slope of the line gives the value of $d \ln b / d \ln V$.

At high temperatures ($0.2\Theta < T < \Theta$) we can plot γ_T against t defined in equation (3.1.22) and fit the curve as $t \rightarrow 0$, by a polynomial equation in t . From this polynomial equation one obtains the value of $\gamma_\infty = \gamma(0)$. If the polynomial equation is rewritten in terms of powers of T^{-2} one could obtain $\gamma(2)$, $\gamma(4)$, etc. The errors in estimating the $\gamma(2n)$ values are obviously inter-related because the value of $\gamma(0)$ is used in obtaining the value of $\gamma(2)$, and the values of $\gamma(0)$ and $\gamma(2)$ are used in obtaining $\gamma(4)$, etc.

To find $\gamma(n)$ for $-3 < n < 0$, the following procedure is adopted. From equation (3.1.9)

$$\begin{aligned} \int_0^\infty \frac{\partial V}{T^{n-1}} \cdot dT &= k \sum_{j=1}^{3p} \sum_{i=1}^N \gamma_{ji} \int_0^\infty \sigma_{ji} \cdot T^{n-1} \cdot dT \\ &= k \sum_{j=1}^{3p} \sum_{i=1}^N \gamma_{ji} \cdot \left(\frac{h}{k} \cdot \omega_j(q_i) \right)^n \int_0^\infty \frac{x_{ji}^{1-n} \cdot \exp(x_{ji})}{[\exp(x_{ji}) - 1]^2} \cdot dx_{ji} \\ &= \left(\frac{h}{k} \right)^n k \sum_{j=1}^{3p} \sum_{i=1}^N \mathcal{J}_{1-n}(\infty) \cdot \gamma_{ji} \cdot \omega_j^n(q_i) \quad (3.3.14) \end{aligned}$$

where

$$\mathcal{J}_n(x) = \int_0^x [\xi^n \exp \xi / (\exp \xi - 1)^2] d\xi$$

is given by Wilson ("Theory of Metals", p. 336, Cambridge Univ. Press, 1953). Similarly

$$\int_0^\infty C_{vhar} \cdot T^{n-1} \cdot dT = \left(\frac{h}{k} \right)^n k \sum_{j=1}^{3p} \sum_{i=1}^N \mathcal{J}_{1-n}(\infty) \cdot \omega_j^n(q_i) \quad (3.3.15)$$

By definition

$$\gamma(n) = \frac{\int_0^\infty \frac{\partial V}{T^{n-1}} \cdot dT}{\int_0^\infty C_{vhar} \cdot T^{n-1} \cdot dT} \quad (3.3.16a)$$

$$= \frac{\int_0^{\infty} \gamma_T C_{\text{vib}} T^{n-1} dT}{\int_0^{\infty} C_{\text{vib}} T^{n-1} dT} \quad (3.3.16b)$$

The same procedure used in obtaining the μ_n from Hwang's integral can be used in evaluating the integrals in the above equation.

In the above integrals γ_T and C_v have to be referred to the volume of the crystal at the Absolute Zero. As the volume dependence of γ_T is not known, only the correction for the volume dependence for C_v is made according to equation (3.3.6).

In this way we will be able to obtain $\gamma_0, \gamma(-2), \gamma(-1)$, etc., from the experimental values of γ_T . The number of $\gamma(n)$ that can be determined this way will depend on the accuracy of measurement of expansion coefficient, compressibility and specific heat. In this way Barron et al. (70) analysed the experimental thermal expansion data in the alkali halides NaCl and KCl. They concluded that with the existing data the values of $\gamma(n)$, for negative values of n could be obtained with a fair reliability; but to obtain accurate values of $\gamma(n)$ for positive n , more accurate expansion data are needed.

(c) Use of $\gamma(n)$ to Predict the Volume Dependence of Other Physical Properties

Physical properties which depend on lattice vibrations can be characterised by an equivalent Debye temperature. For example, the specific heat of a crystal near the Absolute Zero is characterised by an equivalent Debye temperature $\Theta_0^{\text{sp.h.}}$. These equivalent Debye temperatures are related in a simple way to the moments of the frequency distribution function. We can define the quantity

$$\omega_D(n) = \left[\frac{(n+3)}{3} \cdot \mu_n \right]^{1/n} \quad (3.3.17)$$

$\omega_D(n)$ is the Debye cut-off frequency of a Debye spectrum which has an n th moment μ_n . In terms of these $\omega_D(n)$ the following temperatures characterising various physical properties can be expressed:

$\Theta_0^{\text{sp.h.}}$ is the low temperature limit of the equivalent Debye temperature of the crystal characterising its specific heat; it is given by $(h/k)\omega_D(-3)$. $\Theta_{\infty}^{\text{sp.h.}}$ is the high temperature limit of the equivalent Debye temperature of the crystal characterising its specific heat; that is given by $(h/k)\omega_D(2)$.

Θ_{∞}^S is the high temperature limit of the equivalent Debye temperature characterising the entropy of the crystal; it is given by $(h/k)\omega_D(0)$.

Θ_0^{ZE} is the equivalent Debye temperature of a crystal characterising its zero point energy; it is given by $(h/k)\omega_D(1)$.

Θ_0 is the low temperature limit of the equivalent Debye temperature characterising the Debye-Waller factor of the crystal; it is given by $(h/k)\omega_D(-1)$.

Θ_{∞}^M is the high temperature limit of the equivalent Debye temperature characterising the Debye-Waller factor of the crystal; it is given by $(h/k)\omega_D(-2)$.

From the relation

$$\gamma(n) = - \frac{\partial \ln \omega_D(n)}{\partial \ln V} \quad (3.3.18)$$

one can calculate the volume dependence of the different $\Theta - s$ from a knowledge of $\gamma(n)$.

3.4. ELECTRONIC AND MAGNETIC CONTRIBUTION TO THERMAL EXPANSION

In a metal the total contribution to the entropy arises from lattice vibrations, conduction electrons and magnetic interactions. If we write the entropy as

$$S = S_l + S_e + S_m \quad (3.4.1)$$

then the specific heat is given by

$$C_V = T \left(\frac{\partial S}{\partial T} \right)_V = C_{el} + C_{ve} + C_{vm} \quad (3.4.2)$$

The thermal expansion is given by the relation

$$\left(\frac{\partial S}{\partial V} \right)_T = \left(\frac{\partial S}{\partial T} \right)_V \frac{\beta}{\chi_T} \quad (3.4.3)$$

If the different contributions to the entropy are functions $S_i(\Theta_i/T)$ where Θ_i is a characteristic temperature, then

$$\left(\frac{\partial S}{\partial V} \right)_T = \frac{\gamma_i \cdot C_{vi}}{V} \quad (3.4.4)$$

where

$$\gamma_i = - \frac{V}{\Theta_i} \left(\frac{\partial \Theta_i}{\partial V} \right)_T \quad (3.4.5)$$

is the corresponding Grüneisen parameter. We could, therefore, write

$$\beta = \frac{\chi_T}{V} (\gamma_l C_{vl} + \gamma_e C_{ve} + \gamma_m C_{vm}) \quad (3.4.6)$$

It is well known that the conduction electrons in a metal contribute a term to the specific heat proportional to the temperature T . So we should expect in a metal a contribution to thermal expansion coefficient from the conduction electrons which would be linear in temperature. At low temperatures where the lattice contribution to the expansion coefficient varies as T^3 , we could write α as

$$\alpha = BT + DT^3 \quad (3.4.7)$$

By plotting α/T against T^2 the values of B and D can be found. From the value of B and the measured electronic specific heat one could obtain the value of γ_e .

Varley (1110) has derived the following theoretical expression for γ_e .

$$\gamma_e = 1 + \frac{\partial \ln n(E_F)}{\partial \ln V} \bigg|_{E_F, T} - \frac{\mathcal{N}}{n^2(E_F)} \frac{\partial n(E_F)}{\partial E_F} \bigg|_V \left[1 + \frac{\partial \ln \mathcal{N}}{\partial \ln V} \bigg|_{E_F, T} \right] + \frac{C_v}{\beta V n^3(E_F)} \frac{\partial n^2(E_F)}{\partial E_F} \bigg|_V \quad (3.4.8)$$

Here $n(E_F)$ is the number density of states per unit volume at the Fermi level E_F ; \mathcal{N} is the total number of conduction electrons per unit volume in the metal. For a single band free electron model $n(E_F)$ depends only on E_F and

$$\frac{\mathcal{N}}{n^2(E_F)} \frac{\partial n(E_F)}{\partial E_F} = \frac{1}{3} \quad (3.4.9)$$

γ_e for such a case should be $2/3$. Where the single band free electron model is not applicable the value of γ_e can be very different from $2/3$. The magnitude and sign of γ_e will depend on: (1) how rapidly and in what direction $n(E_F)$ varies with energy at the Fermi level; and (2) how sensitive $n(E_F)$ is to changes in volume V . In exceptional cases the electronic Grüneisen parameter could be negative yielding a negative contribution to the thermal expansion coefficient.

In ferromagnetic materials at the Curie temperature and in antiferromagnetic materials at the Néel temperature the onset of ordering of the spins is accompanied by an anomaly in thermal expansion. This effect has been observed in many cases. In such ordered spin arrays at very low temperatures there could be excitations involving spin reversal on a few of the atoms. These excitations are called *spin waves* and when quantized these elementary excitations go under the name of *magnons*. It is well known (Kittel, 552) that in ferromagnetic and ferrimagnetic materials these spin waves obey a quadratic dispersion law: $(\omega(\mathbf{q}) \propto q^2)$ and yield a magnon contribution to the heat capacity varying as $T^{3/2}$

at low temperatures. This magnon contribution to the heat capacity has been observed by Shinozaki (1698) in Yttrium iron garnet (YIG) and Kouvel (1461) in magnetite. In ferromagnetic metals this contribution is superposed on the electron contribution to the specific heat and it becomes difficult to separate the two effects. In ferrimagnetic materials the electronic contribution is absent and the magnon contribution can be easily detected. Magnons must also contribute to the thermal expansion of these materials. The corresponding Grüneisen parameter is a measure of the volume dependence of the effective exchange interaction determining the quadratic dispersion relation in the materials. Lord (657) has discussed the magnitude of the magnon contribution to thermal expansion in Yttrium iron garnet and Europium oxide. He concludes that in YIG it may be just possible to detect the magnon contribution around 4°K; but in Europium oxide the effect is very considerable and should be easily observable with the existing experimental techniques. These measurements can be correlated with the measurements of the pressure dependence of the transition temperature in these materials.

In an antiferromagnetic material, on the other hand, one gets a linear dispersion relation if the anisotropic magnetic energy is neglected in comparison with the exchange energy. In such a case the magnon contribution to the low temperature specific heat varies as T^3 . Since the lattice contribution at these low temperatures also has the same temperature dependence it would not be possible to separate the magnon contribution unless the Néel temperature is low compared to the Debye temperature. In such a case the magnetic contribution will be several times the lattice contribution which can be calculated from the elastic constant data. If the anisotropy energy is not negligible, then the dispersion relation is modified and there is a finite energy gap. In such a case the specific heat at low temperatures varies faster than T^3 . One would expect such a behaviour in $\text{CuCl}_2 \cdot 2\text{H}_2\text{O}$ in which the Néel temperature is about 4°K and the anisotropy energy is half as much as the exchange energy. However, Peterson & Phillips (1604) have only observed a T^3 dependence of the magnon heat capacity in this material. One would expect a similar contribution to the thermal expansion in the antiferromagnetic materials. There are no experiments so far on the magnon contribution to thermal expansion in ferro-, ferri-, and antiferro-magnetic materials.

3.5. COMPARISON BETWEEN THEORY AND EXPERIMENT

(a) Metals

The expansion coefficient of a number of metals has been determined down to $\Theta/20$ by several investigators (Andres, (14, 15, 16, 17, 18, 19, 20,

21); Cart, (162-165); White, (1138, 1139, 1141, 1142, 1143, 1145-1150, 1796, 1797). In most of the metals the low temperature expansion coefficient could be resolved into a lattice term varying as T^3 and an electronic term varying as T . The lattice Grüneisen parameter and the electronic Grüneisen parameter for a number of metals are given in Table 3.1. They are taken from a table compiled by Collins & White (194).

For all the above metals the lattice Grüneisen parameter γ_T varies only slightly with temperature. Except for aluminium and platinum, the lattice Grüneisen parameter for all other metals decreases with decreasing temperature.

Apart from the metal copper for which the electronic Grüneisen parameter is close to the single band free-electron value of 0.67, for most of the metals investigated the electronic Grüneisen parameter has a large value—around 2—and it is positive. From Varley's (1110) analysis, this means that the number density of states at the Fermi level is strongly dependent on volume. For silver and tungsten, on the other hand, the electronic Grüneisen parameters are very small.

White (1150) has determined the thermal expansion of iron-nickel alloys containing 30% nickel and above. These alloys exhibit a negative expansion coefficient at low temperatures. The linear term in temperature is large and negative corresponding to a negative γ value. It is not possible to say how much of this γ is electronic in origin and how much is due to the magnetic interaction of the spins. However, the large negative

value of γ in iron corresponds to the large negative value of the pressure coefficient of its transition temperature suggesting a large magnetic contribution to thermal expansion. A similar explanation may be valid for the large negative $\gamma_{e,m}$ value observed in Chromium (White, 1140). White (1144) has also carried out measurements of the expansion coefficients of dilute alloys, of Mn with copper. Specific heat measurements (Zimmerman & Hoare, 1182) indicate that there is an anomalously large specific heat associated with alignment of the spins of Mn ions, and that this heat capacity is proportional to T at low temperatures. White has observed a similar anomalous expansion varying linearly in temperature and the magnetic Grüneisen parameter was found to be 3.2 ± 0.2 .

There have been some theoretical calculations of the Grüneisen parameter of metals. We consider some of the recent work in this area.

Sharma & Singh (970) used the Cheveau's (1281) model for a metal. In this model the ion-ion interaction, assumed to be central, is characterised by two adjustable parameters representing the first and second derivatives of the potential. The electron interaction is taken into account using linearised Thomas-Fermi theory. The advantage of this model is that the entire potential is invariant to translation and the equilibrium condition is satisfied. Sharma & Singh (970) used the measured second-order elastic constants (SOE) and their pressure derivatives to compute the Grüneisen parameters of individual modes and hence the temperature variation of the effective Grüneisen function γ_T . A comparison with experiment does not reveal a good enough agreement for the BCC metals lithium, sodium and potassium where experimental data on thermal expansion are also meagre (Schouten & Swenson (1679) recently studied potassium). These authors carried out calculations for aluminium and the noble metals, copper, silver and gold. In the case of aluminium the theoretical curve gives a monotonic decrease of γ_T with decreasing temperature, while experiment reveals a minimum in γ_T vs. T curves (?). In the case of copper the calculations using Daniels' (1303) values of the pressure derivatives of the SOE constants are in better agreement with experiment than the calculations using the measurements of Hiki et al., (1409) of the pressure derivatives of SOE constants. Similar is the situation in silver where the calculations using the values of Hiki, Thomas & Granato are much higher than the measured values. These conclusions have also been confirmed by Feldman & Skelton (1337). These authors took the values of the second-order interaction parameters for copper and silver from the measured dispersion data and assumed that anharmonicity need be considered only for the nearest neighbour interaction. In the case of gold, Sharma & Singh (970) found the experimental data

TABLE 3.1. Lattice and Electronic Grüneisen parameters for a number of metals in the cubic system

Metal	γ_{298}	γ_0	γ_e
Ag	2.4	2.2 ± 0.1	—
Al	2.35	2.65 ± 0.15	1.8 ± 0.1
Cu	2.00	1.69 ± 0.05	0.9 ± 0.4
Fe	1.7	1.5 ± 0.4	2.1 ± 0.2
Mo	1.7	1.4 ± 0.3	1.5 ± 0.3
Nb	1.6	1.3 ± 0.2	1.5 ± 0.2
Ni	1.86	1.65 ± 0.1	2.0 ± 0.1
Pb	2.65	2.7 ± 0.2	1.7 ± 0.5
Pd	2.3	2.3 ± 0.2	2.1 ± 0.1
Pt	2.5	3.0 ± 0.3	2.4 ± 0.2
Ta	1.7	1.5 ± 0.2	1.3 ± 0.1
V	1.2	1.0 ± 0.2	1.65 ± 0.1
W	1.6	1.5 ± 0.3	0.2 ± 0.2

to lie in between the calculated curves using the values of pressure derivatives reported by Hiki, Thomas & Granato (1409) and Daniels' values. It may be pointed out here that Kos et al. (1459) have observed an anomalous thermal expansion of gold below 80°K. Martin (1518) had observed that the specific heat of gold shows an anomalous temperature dependence below 8°K. Kos et al. have pointed out that the deviations from the T^3 dependence found in the specific heat and thermal expansion are in opposite directions. No explanation has been proposed for this anomalous behaviour.

There have been some calculations of the Grüneisen parameters of the alkali metals and aluminium from a model pseudopotential by Wallace (1130, 1131, 1791). The modified point ion model potential of Harrison was used. In sodium and potassium overlap interaction of the Born-Mayer type is taken into account between the nearest and the next nearest neighbours. In lithium and aluminium, the overlap interaction is neglected. The parameters of the pseudopotential and the Born-Mayer interaction in the BCC metals were fitted to the equilibrium lattice constant, binding energy and bulk modulus of these metals at 0°K. Wallace then computed the pressure derivatives of the second-order elastic constants which were in reasonable agreement with measurements. The calculations of the Grüneisen parameters reveal some general characteristics:

- (i) The Grüneisen parameters (GP's) for the various lattice modes show a wide range of variation.
 - (ii) The GP's of the LA branch along [100] direction show a rapid drop from the zone centre to the zone boundary.
 - (iii) The Kohn anomalies are also reflected in the GP values. The temperature variation of the effective Grüneisen function γ_T was then computed for sodium and potassium and compared with experiments. For sodium the experimental thermal expansion data were taken from Siegel & Quimby (1703) and for potassium from Monfort & Swenson (1547). The comparison showed that at high temperature ($T \geq 120^\circ\text{K}$) the agreement between theory and experiment was good while at intermediate temperature the calculated values were higher than the experimental values. This clearly points to an overestimate of the Grüneisen parameters of the low and intermediate frequency modes.
- In aluminium also which is face centred cubic the Grüneisen parameters show a wide range of variation and Kohn anomalies are perceived in abundance in the dispersion of the Grüneisen parameters. A comparison with experimental results showed that the calculated values were consistently lower than the experimental values by about 12%.

(b) Rare Gas Solids

Following the pioneering work of Jones and collaborators (268, 269, 270) measurements of many physical properties of solidified rare gases have been made. The thermal expansion of these solidified rare gases have been measured by one of the following methods:

- (i) Bulk density determination (Hinds, 448; Figgins & Smith, Kr, 317; Earwell & Smith, Xe, 289; Manzheli et al., 673, 674, 676).
- (ii) Back reflection X-ray powder photograph method (Bolz & Maurer, Ne, 117; Figgins & Smith, Kr, 317; Earwell & Smith, Xe, 289; Sears & Klug, Xe, 960; Barrett & Meyer, Ar, 62; Peterson, Batchelder & Simmons, Ar, 838).

(iii) Quartz dilatometer method (Manzheli et al., Ar, Kr, Xe, 674).

(iv) Three-terminal capacitance method (Tilford & Swenson, Ar, 1081, Ar, Kr, Xe, 1753; Holste & Swenson, Ne, 1414).

In argon earlier measurements of Dobbs et al. (268) are not in agreement with the other measurements reported in the literature. These other measurements, however, are in general agreement with one another. In Krypton the measurements of Figgins & Smith are in good agreement with the data of Manzheli et al. In Xenon there is again some discrepancy between the results reported by different authors.

The experimental data on solidified rare gases are of interest from a theoretical point of view. The interatomic potential is mainly of two body character and is of the Lennard-Jones form. The interatomic potential parameters appear to be fairly well known. Because of the low melting point of these crystals the zero-point energy is comparable to the static lattice energy and cannot be neglected in computing their equilibrium physical properties. Also the effect of anharmonicity will be more prominent in these materials.

Horton & Leech (456) have made a detailed computation of the vibrational thermodynamic properties of rare gas solids on the basis of Lennard-Jones model. They have studied the effect of varying the exponents of the potential energy and the range of interaction on these properties. Graham (405) has calculated the high and low temperature limits of the Grüneisen parameters in the quasi-harmonic approximation with a 6-12 Lennard-Jones potential. Different values of zero-point energy in relation to the lattice energy were used by him. In all cases he observed that the variation of γ_T with temperature was small amounting only to about 0.025. Leech & Reissland (631) have calculated the expansion coefficients of these materials in the quasi-harmonic approximation with zero-point energy using a 6-12 Lennard-Jones potential. They found

that the theoretical values were higher than the experimental values at high temperatures. Taking cubic and quartic anharmonic terms by perturbation theory in the free energy reduces the discrepancy. Manzheli et al. (674) have made a detailed comparison of their results with the theoretical calculations. They found a discrepancy of about 25% between the theoretical calculations of Leech & Reissland on a 6-12 potential and their experimental values for Ar, Kr and Xe. The most accurate measurement of the thermal expansion of argon at very low temperatures by Tilford & Swenson reveals a discrepancy of about 10% between the theoretically calculated Grüneisen parameters by Klein, Horton & Feldman (1452) using a perturbation theoretical approach and the observed values. The measured values are always lower than the calculated values in the range 1°K to 25°K. In Xenon there is a significant drop in the Grüneisen parameter at low temperatures in contradiction to the quasi-harmonic calculations of Graham (405) and Brown (144). Perhaps the Lennard-Jones potential does not adequately represent the inter-atomic interaction in Xenon.

(c) Crystals With Diamond Structure

The thermal expansion of germanium, silicon, diamond and alpha-tin has been studied at low temperatures by several workers. (Gibbons, 380, 381; Novikova & Strelkow, 793; Novikova, 782, 783, 784; McCammon & White, 702; Carr, McCammon & White, 164; Sparks & Swenson, 1024). The earlier studies indicated that the expansion coefficients of these crystals became negative below certain temperatures. Blackman (107) had anticipated such a behaviour in open structures. However, Daniels (215, 216) calculated the low temperature limit of the Grüneisen parameter in germanium and silicon from measured pressure dependence of the second-order elastic constants. He found positive values of γ_0 for both these crystals and concluded that the expansion coefficients of these crystals should become positive as one approaches the Absolute Zero. Collins (191) made a detailed calculation of the Grüneisen parameters for the acoustic modes in different directions in these crystals. He found positive values of γ_0 for these crystals. McCammon & White (702) confirmed experimentally the conclusion of Daniels. With improved technique for the coating of specimens with silver, Carr, McCammon & White (164) have obtained reproducible values for the expansion coefficients of germanium and silicon down to about 10°K. The effective Grüneisen parameters for these crystals become positive below about 14°K. They seem to approach the limiting values calculated by Collins & Daniels. The minimum value of γ_T observed in germanium is -0.1 and in silicon is -0.4.

While the high temperature limits of γ_T calculated by Collins (191) on the anisotropic continuum model are in reasonable agreement with experiment, the anisotropic continuum model cannot explain the observed expansion in germanium and silicon. According to the calculations of Collins, there is no acoustic mode with a negative Grüneisen parameter in germanium; the mode having the lowest value of γ in silicon is the transverse acoustic mode along the [110] direction, the value of the Grüneisen parameter being -0.12. On the anisotropic continuum model the effective Grüneisen parameter γ_T can never be smaller than the smallest value of the gammas for the different acoustic modes. So this model cannot account for the negative expansion in germanium and the minimum value of γ_T in silicon. Merely assigning a dispersion law to the modes as was done by Sharma & Joshi (968) does not resolve the difficulty.

The dispersion relations in germanium and silicon have been measured along the symmetry directions by inelastic neutron scattering (Brookhouse & Iyengar, 140; Brookhouse, 139). These dispersion curves differed significantly from the calculations of Hsieh (474) on a point atom model with nearest neighbour interaction. In fact the frequencies of the transverse acoustic modes along the [100] direction at the zone boundary are only 60% of the calculated values. The discrepancy arises because of the neglect of long range interactions between the electric dipoles generated on various atoms when they are displaced. Cochran (183) has taken these long-range interactions in the frame work of the shell model and was able to obtain a good agreement between calculated and measured dispersion data. Bienenstock (98) has made an attempt to explain the thermal expansion of germanium using the following approach. Along the symmetry directions one could write the frequencies ω of the transverse acoustic modes as

$$\omega^2(\vec{q}) = \omega_{NW}^2(\vec{q}) - \omega_{DP}^2(\vec{q})$$

where ω_{NW} are the frequencies obtained on Hsieh's nearest neighbour point atom model in the germanium lattice, and ω_{DP} are the corrections arising from the long-range dipole-dipole interactions. The nearest neighbour point atom model in the germanium lattice contains two second-order force constants k_1, k_2 . The values of these force constants as well as their volume derivatives can be obtained from the elastic constants and their pressure derivatives. ω_{DP}^2 goes to zero as $\vec{q} \rightarrow 0$. The values of ω_{DP}^2 for different wave vectors of the acoustic modes are obtained by subtracting the experimental values of ω^2 (from neutron scattering) from the theoretically calculated ω_{NW}^2 . The long-range contribution ω_{DP}^2 is assumed to vary as an inverse power V^{-n} , where V is the volume. The

Grüneisen parameter of any acoustic mode, $\gamma_j(\bar{q})$, is now found from the relation

$$\gamma_j = -\frac{V}{2\omega_j^2} \left[\frac{\partial \omega_{KN}^2}{\partial V} - \frac{\partial \omega_{LD}^2}{\partial V} \right] \quad (3.5.1)$$

This way it was found that $\gamma_j(\bar{q})$ for the TA modes indeed decreases rapidly as \bar{q} increases and becomes negative at the zone boundary. The long-range dipole-dipole force is responsible for this dispersion in $\gamma_j(\bar{q})$. The optical branches were approximated by an Einstein term with a Grüneisen parameter $\gamma_{opt} = 1.29$. The expansion coefficient calculated on this model was in fair agreement with the measurements of McCammon & White (702) when n was chosen to be about 1. Bienenstock's calculations reveal the importance of the optical modes in determining the effective Grüneisen parameter even at low temperatures. Though the optical modes contribute only a few per cent to the specific heat of this crystal at these temperatures, their influence on the effective Grüneisen parameter is large because (i) the Grüneisen parameter of the optic modes is large; and (ii) the Grüneisen parameters of the acoustic modes annul one another. The agreement of the high temperature limit γ_∞ of the effective GP with the calculations on the anisotropic continuum model of Collins (191) is fortuitous.

Dolling & Cowley (271) made exhaustive calculations of the thermodynamic and optical properties of germanium and silicon. They used a Cochran shell model with interactions extending up to second neighbours and obtained the coupling parameters in the model with the measured dispersion curves. In order to evaluate the Grüneisen parameters for the different modes, it was assumed that the anharmonic potential energy arose only from a two body force between nearest neighbours. This involved two parameters which were adjusted to give a reasonable agreement with measured thermal expansion. This model gave results similar to Bienenstock's calculations, with transverse acoustic modes showing negative Grüneisen parameters at the zone boundary.

This model is, however, subject to the following criticisms. The Grüneisen parameters of the transverse acoustic modes in the [111] direction in germanium are about 1.5 to 2 times the values calculated from the measured pressure derivatives of the second-order elastic constants. Srinivasan (1038) has worked out the number of second- and third-order coupling parameters for the germanium lattice when the interactions extend up to second neighbours. All the invariance conditions on the potential energy were applied. It was found that if only nearest neighbour interactions are considered there are two second-order parameters and one third-order coupling parameter. But this model cannot explain the

measured third-order elastic constant of germanium and silicon. This is the reason for the discrepancy between the GPs for the transverse acoustic modes calculated from the model of Dolling & Cowley and from the pressure dependence of the elastic constants, because Dolling & Cowley considered only the anharmonic interaction between the nearest neighbours. If forces extending up to second neighbours are taken into account then there are six second-order and thirty-five third-order coupling parameters (not all of them independent). We can, of course, reduce the number of independent parameters by setting some of them equal to zero. But this has to be done in such a way that the invariance conditions on the potential energy are not violated. It is doubtful whether the model of Dolling & Cowley satisfies this restriction. So we are forced to conclude that the good agreement between theory and experiment of the thermal expansion coefficient with the model of Dolling & Cowley is fortuitous.

Recently Vasiliev et al. (1775) have proposed a very simple model for the diamond lattice. In this model in addition to assuming the first and second neighbour interaction to be central, the bond between two atoms is likened to two rods which are bound to each other by springs placed at a distance from each atom. This gives the freedom for the two halves of the bond to rotate relative to each other. The value of the spring constant and the position of the springs are two additional parameters. With four parameters a good fit was obtained to the dispersion curves of germanium. Using the pressure derivatives of the second-order elastic constants, the pressure derivatives of the force constants were obtained. The computed curve for the temperature dependence of the Grüneisen parameter showed good agreement with experiment.

(d) Ionic Crystals

(i) Crystals With Rocksalt Structure

The thermal expansion of a number of alkali halides belonging to the rocksalt structure has been the subject of extensive investigations in recent years. The interest evinced in these crystals arises from the following reasons. The specific heats of many sodium and potassium halides have been measured accurately down to very low temperatures and these measurements have been analysed in detail theoretically. The adiabatic elastic constants of the sodium and potassium halides have been measured as a function of temperature from liquid helium temperature upwards and the pressure dependence of the elastic constants has been determined at room temperature for some of them. The lattice dynamics of the alkali halides have been the subject of extensive theoretical and experi-

mental investigations and physically reasonable models for the interatomic forces in these crystals have been worked out from a study of the dispersion relations from inelastic scattering of neutrons in these materials.

The interferometric method has been employed by Rubin et al. (922); Yates & Panter (NaCl, KCl, KBr, KI, LiF, 1166); James & Yates (RbBr, NaF, CsI, 498, 499, 500) and by Cooper & Yates (RbCl, 1293) to study the expansion from 20°K to 273°K. White (1141, 1146, 1151) has used his three-terminal capacitance dilatometer to measure the expansion coefficients in LiF, NaCl, NaI, KCl, KBr, KI, CsBr and RbI from about 4°K to 30°K, 55°K to 90°K and 273°K. Meincke & Graham (718, 719) used the Fabry-Perot interferometric technique to measure the expansion coefficient of NaCl, NaI, KCl, and KBr from 7°K to 273°K. In the experiments of White, and Meincke & Graham, the specimens were about 5 cm long. The long length of the specimen enabled them to carry out measurements down to liquid helium temperature with a fair degree of accuracy. A change in length of 2 Å was detectable with their technique. Schuele & Smith (958) have used the back reflection technique to measure the expansion of RbI down to 20°K.

There is in general a fair degree of agreement between the different measurements. For example, the values of Meincke & Graham on the linear expansion coefficient of NaCl and KBr below 20°K are in good agreement with White's measurements. In NaI and KCl, however, the values of Meincke & Graham are systematically lower than White's values by about 7 to 14%. Similar agreement is found between the results of Yates & Panter and those of White, and Meincke & Graham. In sodium chloride Meincke & Graham gave values which disagree by about 20% with the values of Yates & Panter at 40°K. The agreement improves as the temperature increases. The most glaring discrepancy occurs in RbI at low temperatures between the measurements of Schuele & Smith (958) and White (1151). The expansion of RbI needs to be studied carefully to settle this disagreement.

Some definite conclusions can be reached from these studies: The Grüneisen parameter

$$\gamma_r = \frac{\beta V}{\chi_s C_p} \quad (3.5.2)$$

is nearly a constant above a temperature $T \approx 0.2\Theta_D$, where χ_s is adiabatic compressibility, C_p is specific heat at constant pressure, Θ_D is the Debye temperature of the crystal. Between $\Theta_D/5$ and $\Theta_D/10$ the Grüneisen parameter γ_r decreases rapidly in all the alkali halides except LiF. Below a temperature $T = \Theta_D/20$, White observed that the expansion coefficient could be fitted to an equation of the type

$$\alpha = DT^3 + ET^5 + \dots \quad (3.5.3)$$

The equivalent Grüneisen parameter γ_r appears to attain a constant value γ_0 below $\Theta_D/20$ according to White. However, Meincke & Graham are of the opinion that in NaCl the Grüneisen parameter appears to increase below 15°K though they are careful to point out that further measurements are needed to settle the point.

The above general features of the expansion coefficient of the alkali halides are in agreement with theoretical predictions. In 1955 Barron (64) had predicted an abrupt variation in γ_r for a crystal below $0.2\Theta_D$. This agrees with the observations of White, and Meincke & Graham. Blackman (106, 107) has studied the temperature dependence of two-dimensional and three-dimensional ionic lattice of rock salt structure and Barron (65) has studied the case when the masses of the ions are equal. In both these calculations, the overlap interaction between nearest neighbours was assumed to vary inversely as the n th power of the distance between the ions. Blackman finds that the individual Grüneisen parameters for the transverse vibrations show a wider range of variation than the Grüneisen parameters of the longitudinal vibrations. Also some of the transverse vibrations have negative values of γ_r . Barron's calculations with $n = 8$ lead to similar conclusions. In particular the transverse acoustic waves play a dominant role. This results in γ_0 being less than γ_∞ , which is the arithmetic mean of all the Grüneisen parameters. On his model Barron found that γ_r should vary from 1.67 at high temperatures to 1.00 at low temperatures. Varying the repulsive exponent, n , changes the values of γ_0 and γ_∞ , but still $\gamma_0 < \gamma_\infty$. So the experimentally observed decrease in γ_r value with decreasing temperature is a confirmation of theoretical expectations.

Sheard (984), Collins (191), Schuele (957) and Brugger et al. (150) have attempted to calculate γ_0 and γ_∞ of some alkali halides from the measured pressure dependence of the second-order elastic constants on the anisotropic continuum model. While only the elastic waves contribute to γ_0 , γ_∞ arises due to the acoustic as well as optical vibrations of all wave vectors. The anisotropic continuum model does not take into account the dispersion of the acoustic branches and ignores the presence of the optical branches of vibration in the sodium chloride lattice. Table 3.2. gives the experimentally observed values of γ_0 and γ_∞ for some alkali halides reported by White. In the same table are collected the values of γ_0 and γ_∞ calculated by Schuele (957) on the anisotropic continuum model from the pressure dependence of the second-order elastic constants. The ratios c_{44}/c_{11} , $2c_{44}/(c_{11} - c_{12})$ and dc_{44}/dp are also given for these crystals. Actually in the calculation of γ_0 one should use the pressure dependence of the second-order elastic constants at the Absolute Zero.

TABLE 3.2a. γ_0 and γ_∞ values of a few alkali halides from thermal expansion measurements (White, 1151) and from the anisotropic continuum model (Schneide quoted by White).

Crystal	From expansion data		Anisotropic Continuum		$\frac{c_{44}}{c_{11}}$	$\frac{2c_{44}}{(c_{11} - c_{12})}$	$\frac{dc_{44}}{dp}$
	γ_0	γ_∞	γ_0	γ_∞			
LiF	1.70	1.58	1.85	1.66	0.56	1.9	1.9
NaCl	0.90	1.57	1.09	1.51	0.26	0.72	0.34
NaI	1.04	1.71	—	—	—	—	—
KCl	0.32	1.45	0.31	1.06	0.16	0.37	-0.42
KBr	0.29	1.49	—	—	—	—	—
KI	0.28	1.47	—	—	—	—	—

From table 3.2a. we see that the anisotropic continuum model is able to account for the measured γ_0 values fairly well. The higher value of γ_0 for NaCl from the anisotropic continuum model may be real if Meincke & Graham's observations of an increase in γ_r below 15°K are true. In this case γ_0 value quoted by White would correspond to the minimum in the γ_r curve. The observed T³ behaviour of the expansion coefficient would be analogous to the pseudo-T³ behaviour in the specific heat. However, measurements at lower temperatures are needed to settle this point. The fact that the anisotropic continuum model which neglects the existence of the optical branches in the spectrum yields reasonable values of γ_∞ can only be taken as a fortuitous coincidence. One significant fact emerges from table 3.2a. The value of γ_0 increases significantly as the size of the cation decreases. There is a parallel variation in the ratio of c_{44}/c_{11} and in the elastic anisotropy factor. As the size of the cation decreases, the next nearest neighbour interaction between the anions becomes more and more important. This increases the shear wave velocity $(c_{44}/\rho)^{1/2}$ and also the anisotropy factor. The shear wave of the above velocity has the smallest Grüneisen parameter in the alkali halide lattice. As the size of the anion decreases the Grüneisen parameter increases and at the same time, because of the increase in c_{44} , its effect in determining γ_0 becomes less dominant. Therefore, γ_0 increases with a decrease in the size of the cation.

Table 3.2b. gives a more recent compilation (White & Collins, 1802) of the values of γ_0 from thermal expansion data for several alkali halides having the NaCl structure. There is a slight difference in the values of γ_0 calculated from elastic constant data, the reason being that more recent and accurate data on the elastic constants and their pressure derivatives are used in this compilation.

A detailed analysis of the γ_r curves in NaCl and KCl have been made

TABLE 3.2b. γ_0 values for a few alkali halide crystals from thermal expansion and elasticity data compiled by White & Collins (1802)

Crystal	Expansion data		Elastic Constant data		$\frac{dc_{44}}{dp}$ (R.T)	$\frac{2c_{44}}{c_{11} - c_{12}}$ (°K)
	γ_0	γ_∞	γ_0	γ_∞		
LiF	1.7	1.65	1.65	1.4	1.57	0.68
NaF	0.92	0.99	1.02	0.21	0.58	0.56
NaCl	1.04	1.06	1.13	0.37	0.54	0.31
NaBr	0.99	1.03	0.33	0.42	0.29	0.23
NaI	1.03	1.26	0.05	0.59	0.27	0.24
KCl	0.35	0.33	0.36	-0.39	0.20	0.84
KBr	0.29	0.36	0.34	-0.33	0.24	0.27
KI	0.28	0.34	0.05	-0.24	0.59	0.51
RbCl	0.00	0.05	-0.05	-0.61	3.7	0.84
RbBr	-0.03	-0.05	-0.18	-0.59	2.1	2.2
RbI	-0.11	-0.18	1.09 to 2.1	-0.51	3.7	0.84
CsBr	2.02	2.1	2.0 to 2.2	3.7	0.8	
CsI	1.93	2.0	2.0 to 2.2	3.7	0.8	

by Barron, Leadbetter & Morrison (70) using White's experimental data to give the quantities $\gamma(-3)$, $\gamma(-2)$, $\gamma(-1)$, $\gamma(0)$, $\gamma(2)$, $\gamma(4)$ and $\gamma(6)$. Meincke & Graham have carried out a similar analysis to obtain values of $\gamma(2)$, $\gamma(4)$ and $\gamma(6)$ for NaCl, NaI, KCl and KBr. A similar analysis has been carried out in RbCl by Cooper & Yates (1293) and their values are also included in table 3.3.

From table 3.3. it is observed that, except in the case of RbCl, $\gamma(n)$ appears to have a maximum at $n = 2$. Using Kellerman's rigid ion model with nearest neighbour central interaction, Barron calculated $\gamma(n)$ for the case where the two ions are of equal mass and the exponent in the overlap interaction has a value $n = 8$ and $n = 10$. This model also gave a variation of $\gamma(n)$ having a maximum around $n = 2$. Meincke & Graham (719) have extended the model by taking into account the mass differences of the ions and including central overlap contributions between all neighbours. They found that the observed values of $\gamma(0)$, $\gamma(2)$, and $\gamma(4)$ can be reasonably well fitted by taking a value of n between 8 and 10 for the different alkali halides. However, for any given model the theoretically calculated $\gamma(n)$ varied more rapidly than the observed values.

The case of lithium fluoride stands apart from the other alkali halides. In LiF, the Grüneisen parameter increases with decreasing temperature. The large deviation from Cauchy relations in LiF indicates that the

TABLE 3.3. Values of $\gamma(n)$ for a few alkali halides obtained by an analysis of thermal expansion data

$\gamma(n)$	NaCl	NaI	KCl	KBr	RbCl
$\gamma(-3)$	0.95 ± 0.10^a		0.31 ± 0.03^a		0.35 ± 0.30^a
$\gamma(-2)$	1.25 ± 0.04^a				0.70 ± 0.05
$\gamma(-1)$	1.44 ± 0.04^a				1.40 ± 0.12
$\gamma(0)$	1.59 ± 0.01^a		1.44 ± 0.01^a		1.46 ± 0.12
	1.58 ± 0.01^b	1.74 ± 0.01^b	1.45 ± 0.01^b	1.49 ± 0.01^b	
$\gamma(2)$	1.74 ± 0.08^a		1.65 ± 0.09^a		
	1.83 ± 0.05^b	1.92 ± 0.05^b	1.66 ± 0.05^b	1.55 ± 0.05^b	1.95 ± 0.30
$\gamma(4)$	1.7 ± 0.2^a		1.41 ± 0.2^a		
	2.0 ± 0.2^b	1.70 ± 0.15^b	1.55 ± 0.3^b	1.35 ± 0.01^b	2.56 ± 0.62
$\gamma(6)$	1.6 ± 0.5^a		0.7 ± 0.5^a		

^a Barron et al. (70)^b Meinecke & Graham (718, 719)^c Cooper & Yates (1293)

overlap forces are non-central. Magnesium oxide bears a close similarity to lithium fluoride. White & Anderson (1153) have measured the expansion of MgO down to about 20°K and conclude that in this crystal also γ_T appears to increase slightly as the temperature is reduced. They give the value of γ_∞ as 1.5 and γ_0 as 1.6. The expansion coefficient of MgO is very small and so the errors of measurement at low temperatures are correspondingly large. Ganesan (369) anticipated the increase in γ_T in MgO with decreasing temperature and showed that such a behaviour was to be expected on a theoretical model involving non-central forces. Assuming a V^{-3} volume dependence for the non-central forces, he found that the transverse acoustic branch along [100] has a γ value 1.0 in contrast to the negative value for sodium chloride lattices with a central interaction. The range of variation of γ between the different acoustic waves is less and since the difference between the longitudinal and transverse wave velocities is not as large as in the sodium chloride lattice with central interaction, the value of γ_0 is not much overweighted towards the modes having the smallest GP values.

Detailed calculations of the temperature dependence of γ_T for the NaCl lattice have been carried out by Arenstein, Hatcher & Neuberger (30) using the Kellerman rigid ion model with nearest neighbour central overlap interaction. These authors employed an inverse power form for the repulsive interaction as well as an exponential Born-Mayer form. The Grüneisen parameters for the individual modes were obtained using a perturbation procedure. The volume dependence of the Grüneisen parameters was also taken into account. The γ_T versus temperature

curves calculated by Arenstein et al. exhibited a well defined minimum at low temperatures. However, as Achar & Barsch (1189) have pointed out these calculations are of dubious value because the equilibrium condition was not used in fixing the parameters. Achar & Barsch (1189) made a very careful calculation of the variation of $\gamma(n)$ for the rocksalt crystal using a negative ion polarisable rigid shell model with general first neighbour interaction and axially symmetric next nearest neighbour anion-anion interaction. The measured pressure derivatives for the three second-order elastic constants were used in obtaining the third-order anharmonic parameters of the overlap interactions. They also used (i) the rigid ion model (RIM) with nearest neighbour central forces satisfying the equilibrium condition and (ii) a modified rigid ion model (MRIM) with general nearest neighbour interaction and axially symmetric next nearest neighbour anion-anion interaction. The salient differences between the shell and rigid ion model calculations were:

- (i) the total spread of the Grüneisen parameters for the various normal modes is 25% smaller in the shell model than in the rigid ion model;
 - (ii) the negative values of the Grüneisen parameters at small wave vectors for the TA branch along [100] and [110] obtained on the RIM are raised and become positive when the shell model (SM) is used. However, this is not an effect due to the inclusion of the polarisability of the ions but due to the extension of the overlap interaction to second neighbours;
 - (iii) the GP for the TA mode polarised in the XY plane for wave propagation along [110] direction is lowered in the SM compared to the RIM; and
 - (iv) the GP for the LA mode along the [111] direction is higher in the shell model than in the RIM.
- The experimental $\gamma(V, T)$ data of White (1152) were reduced to constant volume γ_0 by using the expression

$$\gamma(V, T) = \gamma(V_0, T) \left[1 + \frac{\partial \ln \gamma}{\partial \ln V} \right]_{T} \frac{V - V_0}{V_0} \quad (3.5.4)$$

where for the constant $\frac{\partial \ln \gamma}{\partial \ln V}$ the value calculated by Roberts &

Ruppin (1651) was used. These reduced data were compared with the calculations on the SM, RIM and MRIM. At 0°K the SM calculation gave the correct γ_0 because the parameters were fitted to do so. As the temperature increases the SM calculations increase faster than the experimental values, the discrepancy being 6% at low temperatures and 8.4% at higher temperatures. These calculations indeed reveal a shallow

minimum around 15°K. The minimum is ascribed to the TA modes along [100] having a GP which decreases as one proceeds from the zone centre to zone boundary. Since the parameters in RIM are too few, the calculated low temperature limit γ_0 will not agree with experiment. However, one can observe that in RIM γ_T rises more steeply with temperature than with the shell model. The value of γ_T assumes a constant value γ_0 at lower temperatures than in the shell model. The RIM also shows a weak maximum in γ_T which becomes more pronounced in the MRRM.

The authors have shown that the inclusion of the second neighbour interaction has the effect of increasing γ at low temperatures and depressing γ at high temperatures. The inclusion of polarisability has the opposite effect. At low temperatures the two effects nearly cancel each other and this is the reason why the earlier RIM calculations with nearest neighbour central interactions were successful in explaining the experimental behaviour at low temperatures. On the other hand, at high temperatures the first effect dominates. So a simple RIM without the inclusion of second neighbour interaction will predict too high a value of γ in comparison with experiment at high temperatures.

For the other alkali halides shell model calculations have been made by Cowley & Cowley (211) (for NaI and KBr) and by Nanjoshi et al. (1560) (for all the alkali halides). In the calculations of Cowley & Cowley the parameters of the shell model were evaluated by fitting the measured dispersion relations for NaI and KBr at 90°K. The model used is the Model IV of Cowley which involves interactions up to second neighbours. It is assumed that anharmonic effects arise only from the nearest neighbour overlap interaction and anharmonic effects due to Coulomb interaction are small. Calculations were performed with and without taking into account the anharmonicity of the Coulomb interaction. These authors plot the Grüneisen parameters of the longitudinal and transverse optic branches along [100], [111] and [110] directions as a function of wave vector in KBr. The Grüneisen parameters of the transverse optic branches are almost independent of wave vector in all three directions. But the GPs of the LO branch along [110] and [100] directions increase rapidly as the zone boundary is reached. These observations were also confirmed by the calculations of Ruppin & Roberts (1659). For these directions the GP of the transverse acoustic branch with the wave velocity $(c_{td}/\rho)^{1/2}$ is negative and varies a little with wave vector. The LA branch shows a large dispersion in GP along the [100] and [110] directions. The effect of including the Coulomb interactions is drastic in the TA mode with negative GP along [100] and [110]. The magnitude of the GP is reduced and along the [110] direction the GP changes sign from negative to

positive near the zone boundary. The corresponding curves on the Kellerman's rigid ion model given by Arenstein et al. for NaCl along the [100] direction are significantly different from the curves for KBr given by Cowley & Cowley. The calculated temperature dependence of the Grüneisen parameter in NaI and KBr are compared with the measurements of Yates & Panter (1166), and Meincke & Graham (719). The agreement between theory and experiment is fair.*

In Nanjoshi et al. (1560) calculations the authors have used a negative ion polarisable shell model with general nearest neighbour interaction and central next nearest neighbour anion-anion interaction. This interaction is taken to depend on a single parameter A , though in principle this central interaction should be defined by two parameters. The charge on the positive ion, which is treated as a point charge, is taken to be greater than 1. It is also assumed to vary with volume as $\partial \ln Z / \partial \ln V = 0.5$. However, the authors have not included the contribution from this variation of charge with volume in their expression for the second-order elastic constants. Hence these calculations have not been performed self-consistently. The third-order anharmonic parameters have been obtained from pressure derivatives of the second-order elastic constants, the low and high frequency dielectric constants and the frequency of the transverse optic mode at (000). The GPs calculated show the same trend with wave-vector as in the other calculations. The TA modes along [100] show negative values for KCl and RbI. The negative thermal expansion of RbI at low temperatures is ascribed to this reason. The temperature variation of the Grüneisen function is in fair agreement with experiment.

Ruppin & Roberts (1659) have used a similar shell model for the calculations of GPs of LiF, sodium halides, potassium halides and rubidium halides. They calculated only the high temperature limits of the Grüneisen function. In all the alkali halides the calculated values were greater than the measured values by 0.1. This seems to be the general feature of all the calculations so far. Ruppin (1655, 1656) has calculated the mode Grüneisen parameters and the temperature dependence of the Grüneisen function γ_T in MgO, CaO and SrO. He used a negative ion polarisable shell model with general nearest neighbour interaction and axially symmetric next nearest neighbour interaction. The anharmonic parameters were obtained from the pressure derivatives of the SOE constants and the changes with volume of the optic mode frequencies. In MgO γ_T increases as the temperature is decreased in agreement with experiment. In CaO and SrO, on the other hand, γ_T decreases with decreasing temperature. This difference in behaviour is attributed to changing anisotropy of the elastic constants.

*See Appendix 1, p. 195.

(ii) Crystals With Caesium Chloride Structure

The temperature dependence of the Grüneisen function γ_T in crystals with caesium chloride structure has been studied theoretically by Ganesan & Srinivasan (372). The model used was a point ion model with nearest neighbour central interaction varying as the inverse n th power of the distance. The exponent n was varied from 8 to 30. For $n \leq 7.3$ the CsCl lattice becomes unstable, to a shear elastic mode involving the elastic constant c_{44} . The GPs were calculated for waves propagating in different directions. The TA mode along [110] direction involving the shear modulus $(c_{11} - c_{12})/2$ has the smallest γ value which is negative for $n \geq 15$. The shear elastic mode involving c_{44} has the largest γ value which increases rapidly as n is reduced. The low temperature limit γ_0 was calculated. As the value of n increases γ_0 decreases. For small values of n , the large value of the shear mode along [100] predominates due to the small velocity of this mode. As n increases the elastic anisotropy decreases and all the modes contribute equally to γ_0 . The quantities $\gamma(0)$, $\gamma(2)$, $\gamma(4)$ and $\gamma(6)$ were also calculated. For small values of n (i.e., $n < 16$), $\gamma(n)$ increases monotonically as n decreases. For $n > 16$, $\gamma(n)$ decreases as n decreases. Detailed calculations of the temperature dependence of γ_T reveal that for $n < 15$, the Grüneisen function increases with decreasing temperature while for $n > 20$, it decreases with falling temperature. The ratio of the masses of the ions has no marked influence on the temperature dependence of γ_T . When $n = 16$, the effective Grüneisen parameter is independent of temperature. The solid obeys the Grüneisen's law *exactly*. We have here an example of a perfect Grüneisen solid in Blackman's sense. The measured elastic constants of CsBr and CsI correspond to a value of $n \approx 15$. It was concluded that if this model were applicable, the caesium halides should show little variation in the effective Grüneisen function.

White (1151) has determined the expansion of CsBr from 7° to 30°K, 55–90°K and 273°K using his capacitance dilatometer. Using the elastic constant data of Marshall (685) to arrive at the Debye temperature Θ of this crystal, the Grüneisen parameter γ_T of CsBr below $\Theta/50$ was evaluated by White. He found that the γ_T value was not significantly different from the value at room temperature. Recently Bailey & Yates (51) have measured the expansion coefficients of CsCl, CsBr and CsI from 20°K to 273°K. These authors found that in all these caesium halides the Grüneisen parameter remains almost a constant over the entire temperature range and the Grüneisen parameters for these three halides have almost the same value.

Recently, Vetelino, Mitra & Nanjoshi (1778) calculated the mode

Grüneisen parameters for the caesium halides with a rigid ion model, the change on the ion being an adjustable parameter. Nearest and next nearest neighbour general interaction were taken. The cation-cation and anion-anion second neighbour interactions were assumed to be the same. The anharmonic parameters were obtained from the pressure derivatives of the SOE constants and the optic mode frequencies. The general features were:

- (i) along [100] the LA and LO modes have nearly the same Gamma value and exhibit very little dispersion of the Grüneisen parameter,
- (ii) along [111] the Grüneisen parameter of the TO mode shows a large dispersion from zone centre to zone boundary, and
- (iii) the LO and LA modes along [111] exhibit maxima and minima in the dispersion of their Grüneisen parameters.

These calculations also confirm that the Grüneisen function γ_T is almost independent of temperature down to 10°K but exhibits an appreciable hump below this temperature. As no comparison could be made with dispersion curves, one does not know how good the model is.

Recently White & Collins (1802) have reported measurements on CsCl, CsBr and CsI down to 2°K and they have not observed the pronounced hump in γ_T at low temperatures. They have observed a very small hump around $\Theta/20$, which they attribute to errors in the specific heat data for these two crystals. The pronounced humps in the calculation of Vetelino et al. perhaps arise due to the use of too coarse a mesh in the long wavelength limit.

(iii) Crystals With Zinc Blende Structure

The measurements of Adenstedt (4) revealed that zinc sulphide in the cubic modification exhibits a negative expansion coefficient below –190°C. In 1958 Blackman (107) made a theoretical investigation of an ionic lattice belonging to the ZnS and NaCl structures. Assuming nearest-neighbour overlap interaction varying as r^{-n} , Blackman showed that the transverse elastic waves propagated in most of the directions in ZnS structure have negative GPs. As these transverse elastic waves are dominant in determining the low temperature limit γ_0 , one observes a negative thermal expansion at low temperatures. The negative value of γ_0 is found to occur for two reasonable values of n . In the alkali halides, on the other hand, only the transverse waves associated with c_{44} had a negative Grüneisen parameter and the value of γ_0 became negative only when c_{44}/c_{11} —ratio was made very small by increasing n to a very large value. So Blackman concluded that it was reasonable to expect a negative

volume expansion coefficient in ZnS type of structures, but such a behaviour should be uncommon in alkali halides. Blackman suggested an experimental study of the expansion of a number of crystals having the sphalerite structure to find out if the negative volume expansion coefficient is of common occurrence at low temperatures in these crystals.

Gibbons (380) and Novikova (784, 785, 788) have investigated several compounds having the ZnS structure. Gibbons (380) carried out his measurements down to 4.2°K using the interferometric technique while Novikova could only go down to 20°K with a quartz dilatometer. The crystals investigated were InSb, GaAs, ZnSe, AlSb, GaSb, ZnTe and HgTe. In all these crystals the expansion is positive at room temperature, but it changes sign as the temperature is lowered. In InSb Gibbons observed a minimum in the expansion coefficient around 30°K, the expansivity becoming less negative at lower temperatures. Such minimum was not observed by Novikova for the other materials. The minima for these materials perhaps occur at temperatures lower than 20°K. Novikova concluded that as the ionic character of the bond increases, the temperature at which the change of sign of thermal expansion takes place increases. Blackman's expectation that a negative expansion coefficient at low temperatures must be a common occurrence in crystals of the ZnS structure is thus borne out. Alpha-silver iodide is a crystal belonging to this structure. Earlier investigations of the expansion coefficient of this crystal at room temperature indicated a negative value. However, silver iodide occurs both in the sphalerite and wurtzite structures and one is not sure whether the earlier measurements did not refer to a mixture of both phases in unknown proportions. In 1963, Bienenstock & Burley (99) studied the expansion of silver iodide powder from 4.2°K to 300°K using an X-ray diffraction method. The specimens were prepared in two different ways. Silver iodide powder was heated to melting and then rapidly quenched in water. The resulting specimen was crushed and ground to a fine powder. In the second method of sample preparation, AgI powder was compressed to 3000 bars and the resulting pellet was crushed and powdered. In these methods of sample preparation it is believed that more than 90% of the powder is in the cubic ZnS phase. The expansion measurements on the two different specimens did not yield the same results. However, both the measurements showed that the expansion coefficient is negative below about 70°K and above 120°K. In the range 70° to 120°K the expansion is positive. In accounting for this strange behaviour in AgI, Bienenstock & Burley have some illuminating remarks to make about the expansion of ZnS structures. They point out that the longitudinal acoustic modes and all optical modes have positive Grüneisen parameters since in such modes the nearest neighbour bonds are compressed or extended. On the other hand, those transverse acoustic modes at long wave length in which the planes of atoms move perpendicular to nearest neighbour bonds should have negative Grüneisen parameters. As the wave length decreases the GPs of these modes should show a tendency to become positive depending on the number of nearest neighbours in the plane of atoms. In ZnS this number is small and so the TA modes should have a negative GP even at shorter wavelengths. The more covalent the bond, the more positive is the GP for modes involving the bending of the bonds. In ZnS structures the low temperature limit γ_0 is negative because of the large weightage in favour of the TA modes of long wavelength. At high temperatures the limit γ_∞ is the arithmetical mean of all modes. The positive contribution to the GPs due to LA mode and LO and TO modes is almost balanced by the negative contribution of the TA modes. In crystals where the bonding is more ionic and in which the overlap repulsive exponent n is large one could even get a negative value for γ_∞ ; so the crystals could exhibit a negative expansion at high temperatures. The calculations of Rajagopal & Srinivasan (878) show that as the ionic character of the ZnS structure increases quite a large number of TO modes occur with frequencies lower than the acoustic modes. So at some intermediate range of temperatures these modes play a dominant role in making effective GP positive. So we may find a region of positive expansion sandwiched between two regions of negative expansion as it happens in AgI. The qualitative arguments of Bienenstock & Burley are quite reasonable. However, in the absence of a satisfactory model for the dynamics of these crystals, we are unable to put these ideas on a reliable quantitative basis. Recently Vettori et al. (1119) used a rigid ion model for ZnTe and computed the thermal expansion using experimental data on the pressure variation of SOE constants to fix the anharmonic parameters. How far such a model is applicable to ZnS type materials is still open to question.

(iv) Crystals With Fluorite Structure

The thermal expansion of CaF_2 , SrF_2 and BaF_2 has recently been measured by Bailey & Yates (50) using an interference method down to 20°K. The experimental accuracy at the lowest temperature is around 20%. Using an analysis proposed by Barron et al. (70), Bailey & Yates (50) have utilised their experimental data to obtain the values of $\gamma(n)$ which are tabulated in Table 3.4. Their results clearly indicate a drop in the effective GP, γ_T , with a decrease in temperature.

This result is in sharp contrast with an earlier theoretical calculation of Ganesan & Srinivasan (371) for CaF_2 . These calculations pointed

TABLE 3.4. $\gamma(n)$ for the alkaline earth fluorides

$\gamma(n)$	CaF ₂	SrF ₂	BaF ₂
$\gamma(-3)$	0.8 ± 0.5	0.4 ± 0.03	0.2 ± 0.4
	0.84	0.55	-0.03
Theory			
$\gamma(-2)$	1.58 ± 0.1	1.00 ± 0.06	0.76 ± 0.01
$\gamma(-1)$	1.78 ± 0.1 ₂	1.36 ± 0.0 ₉	1.22 ± 0.0 ₂
$\gamma(0)$	1.83 ± 0.1 ₃	1.64 ± 0.0 ₁	1.58 ± 0.0 ₂
$\gamma(2)$	1.96 ± 0.2 ₃	1.80 ± 0.1 ₀	
$\gamma(4)$	1.98 ± 0.5 ₇		

to a sharp rise in γ_T with decreasing temperature. However, in this calculation the rigid ion model was used and the volume dependence of the force constants were obtained by fitting the observed temperature dependence of c_{44} assuming that the entire temperature dependence arises due to thermal expansion of the crystal. This assumption is not borne out by measurements of the pressure dependence of the second-order elastic constants by Wong & Schuele (1157). Because of this faulty assumption the GPs of the acoustic modes came out too large and hence γ_T value calculated is much larger than the γ_T value observed. Recently, using Axe's shell model, Srinivasan (1039) calculated the third-order elastic constants of these alkaline earth fluorides. The pressure dependence of the second-order elastic constants calculated for these fluorides as well as the individual third-order elastic constants (TOE) calculated by Srinivasan are in fairly good agreement with the measured values. Using the Axe's shell model Srinivasan (1040) calculated the low temperature limits of GP, γ_0 , for all the three alkaline earth fluorides and these values are given in Table 3.4. The agreement with the measured values is satisfactory.

Ruppin (1657) calculated the temperature dependence of the Grüneisen function γ_T in CaF₂ and BaF₂ using Axe's version of the shell model. The third-order parameters of the overlap interaction have been obtained from the pressure derivatives of c_{11} , c_{12} and c_{44} and the pressure dependence of the static and high frequency dielectric constants. The GPs show a large range of variation in the crystal. The calculated γ_T function is in fair agreement in CaF₂ and BaF₂ with the measurements of Bailey & Yates (50). Ramachandran & Srinivasan (1631) carried out similar calculations in the three alkaline earth fluorides. They used the original Axe's shell model in which the overlap interactions were assumed to vary as the inverse power of the distance. No new parameter was introduced in the calculations. Their results are similar to those of Ruppin (1657). In lead fluoride these authors calculated the TOE constants using Axe's shell model and showed that the low temperature limit of γ_T (i.e., γ_0) is negative suggesting strongly that the thermal expansion

of PbF₂ would become negative at low temperatures. The thermal expansion of antiferroelectric compounds Mg₂Si and Mg₂Sn have recently been determined by Novikova (1571) between 25° and 300°K. Their measurements indicate that the linear expansion coefficients of both the compounds may become negative below 20°K.

3.6. THERMAL EXPANSION OF ANISOTROPIC MATERIALS

The thermal expansion of hexagonal metals like zinc and cadmium exhibit considerable anisotropy along and perpendicular to the hexad axis. This fact has been observed as early as 1924 by Grüneisen & Goens (416). In zinc the expansion coefficient perpendicular to the axis becomes negative below 70°K. In recent years the thermal expansion of a number of materials which are uniaxial has been determined down to liquid helium temperature (Meyeroth & Smith, 728; White, 1149, 1794, 1795; McCammon & White, 703; Channing & Weintroub, 171; Bunton & Weintroub, 1263; Bailey & Yates, 1215).

Magnesium has a c/a ratio which is close to that of an ideal hexagonal close packed lattice. The expansion coefficient of magnesium parallel and perpendicular to the axis shows that only a slight anisotropy exists. Zinc and cadmium have an axial ratio far larger than the value for an ideal hexagonal close packed lattice. They also exhibit a marked anisotropy in thermal expansion. The expansion coefficient parallel to the axis is much larger than the expansion coefficient perpendicular to the axis. The value of α_c becomes negative at low temperatures (below 40°K for Cd and 75°K for zinc). This negative expansion perpendicular to the axis is a result of the dominance of the Poisson contraction in this direction accompanying the longitudinal expansion α_l . In zinc a curious oscillatory behaviour in α_c has been observed by McCammon & White (703) in the liquid helium range of temperature. This result needs to be confirmed by other workers. In these materials the Grüneisen parameter γ_T shows a broad hump in a temperature range of about 0.03 to 0.1 Θ_D . The low and high temperature limits of γ_T appear to be not significantly different from each other. In magnesium, there is a slight dip in the γ_T value at about 0.05 Θ_D . Otherwise there is very little change in the value of γ_T .

The thermal expansion of pyrolytic graphite, which is hexagonal in structure, has been measured from 20 to 273°K by Bailey & Yates (1215). The Grüneisen parameters γ' and γ'' were obtained as a function of temperature. γ' was positive at all temperatures and increased in magnitude as the temperature was reduced. γ'' was negative and became more negative at very low temperatures.

*The superscripts ' and ' denote the values of GP perpendicular and parallel to the unique axis, respectively.

Among the trigonal crystals, studies of the thermal expansion of the following materials have been made at low temperatures: quartz (White, 1148); antimony (Buntin & Weintraub, 1263; White, 1794); bismuth (Buntin & Weintraub, 1263; White, 1794, 1795). Dilatometer experiments indicate that in quartz the expansion coefficient perpendicular to the axis α_{\perp} is more than the expansion coefficient α_{\parallel} parallel to the axis, and the latter becomes negative below 12°K. However, the volume expansion coefficient β remains positive down to 4°K. The Grüneisen parameter for alpha-quartz exhibits a hump similar to that in hexagonal metals. This hump occurs at about $T = 0.03 \Theta_D$. However, till about $0.01 \Theta_D$ the Grüneisen function γ_T does not show a tendency to level off to a constant value as it happens in other hexagonal materials. In antimony and bismuth α_{\parallel} is considerably larger than α_{\perp} at all temperatures. α_{\perp} for antimony is negative below 20°K and shows a minimum at 14°K. The Grüneisen γ in bismuth shows a minimum around 8°K and rises at lower temperatures to about 1.8°K. This is similar to the minimum observed in diamond-structure crystals.

Among the tetragonal metals tin and indium have been studied. In tin (White, 1149) the expansion coefficient perpendicular to the axis becomes negative below 25°K. There is a marked anisotropy in the thermal expansion of this metal at low temperatures. Indium shows a negative expansion parallel to the unique axis and a positive thermal expansion perpendicular to the unique axis even at room temperature (Munn, 1556).

Among the compounds belonging to the hexagonal symmetry, the thermal expansion coefficient of ZnO has been studied down to low temperatures. This compound belongs to the Würtzite structure. Soga & Anderson (1021) measured the pressure variation of the elastic constants of powdered specimens of ZnO. These elastic constants are averages over all possible orientations of the grains of single crystal elastic constants. An interesting result was the negative sign of the pressure derivative of the effective shear elastic constant. A calculation of the low temperature limit of the volume Grüneisen parameter yielded a negative value suggesting the possibility of a negative thermal expansion in this material at low temperatures. This has been confirmed by the measurement of α_{\parallel} and α_{\perp} on single crystals of ZnO by Ibach (1419) and Yates et al. (1817). Both the linear expansion coefficients become negative below about 100°K. While γ'' obtained from the experimental data remains positive down to the low temperatures reached, γ' becomes negative at low temperatures. The analysis of the specific heat and thermal expansion data revealed that (i) there is a monotonic decrease in the value of $\omega_D(n)$ as n decreases and the spread of values from $\omega_D(-2)$ to $\omega_D(6)$ is larger than in cubic ionic crystals of the NaCl structure. Similarly $\gamma(n)$ shows a rapid drop as

n decreases. The behaviour is similar to that of cubic zinc sulphide though the analysis in cubic ZnS is not very reliable due to wide disagreement between different sets of data.

Munn (751) has summarised the experimental situation about the thermal expansion of anisotropic materials.

There is very little theoretical work on the thermal expansion of anisotropic materials. Writing the free energy as a function of temperature and the strain components ϵ_{ij} , the following equation can be derived for the components of the linear expansion coefficient tensor

$$V \cdot \alpha_{kl} = k \sum_{mn} s_{kl,mn} \sum_{j=1}^{3p} \sum_{i=1}^N \gamma_{j,li} \cdot \sigma_{j,li} \quad (3.6.1)$$

Here the indices k, l, m, n take on the values 1, 2, 3; α_{kl} are the components of the linear expansion coefficient tensor, $s_{kl,mn}$ are the elastic compliance coefficients in tensor notation and $\gamma_{j,i} \cdot \sigma_{j,i}$ are generalised Grüneisen parameters defined by

$$\gamma_{j,i} \Big|_{mn} = - \frac{\partial \ln \omega(\bar{q})}{\partial \epsilon_{mn}} \quad (3.6.2)$$

where ϵ_{mn} are the strain components. For uniaxial crystals the convenient strain parameters to use are (i) a uniform areal strain ϵ_{\perp} perpendicular to the unique axis and (ii) a uniform longitudinal strain ϵ_{\parallel} parallel to the unique axis. For these crystals the expansion coefficients α_{\parallel} and α_{\perp} are defined by equations (3.6.3).

$$V \cdot \alpha_{\parallel} = k \left[2s_{13} \sum_{j=1}^{3p} \sum_{i=1}^N \gamma_{j,li} \cdot \sigma_{j,li} + s_{33} \sum_{j=1}^{3p} \sum_{i=1}^N \gamma_{j,li} \cdot \sigma_{j,li} \right] \quad (3.6.3a)$$

$$V \cdot \alpha_{\perp} = k \left[(s_{11} + s_{12}) \sum_{j=1}^{3p} \sum_{i=1}^N \gamma_{j,li} \cdot \sigma_{j,li} + s_{13} \sum_{j=1}^{3p} \sum_{i=1}^N \gamma_{j,li} \cdot \sigma_{j,li} \right] \quad (3.6.3b)$$

Here the s_{ij} are again the compliance coefficients in Voigt's notation and

$$\gamma_{j,li} = - \frac{\partial \ln \omega(\bar{q})}{\partial \epsilon_{\perp}} \quad (3.6.4a)$$

$$\gamma_{j,li} = - \frac{\partial \ln \omega(\bar{q})}{\partial \epsilon_{\parallel}} \quad (3.6.4b)$$

The anisotropic thermal expansion of these uniaxial materials can be discussed in terms of the temperature dependence of the effective Grüneisen functions γ_T' and γ_T'' defined in a fashion analogous to the equation (3.1.12). McCammon & White (703) have given plots of γ_T' and γ_T'' as a function of temperature for Mg, Cd and Zn.

The only theoretical work on the thermal expansion of hexagonal materials is due to Srinivasan and coworkers. Srinivasan & Ranji Rao (1042) computed the Grüneisen parameters for a three-dimensional ideal hexagonal close packed lattice with nearest neighbour central interactions of the type

$$\phi(R) = -\frac{\alpha^+}{R^m} + \frac{\beta^+}{R^n}$$

For elastic modes propagating in different directions in the crystal, they found the following results: (i) γ' and γ'' for the elastic modes depend strongly on the direction of propagation. For all modes propagating along the axis of the crystal, γ'' is very large. The value of γ'' decreases rapidly as the direction of propagation deviates away from the hexad axis for one of the transverse, and longitudinal acoustic modes. The γ' value, on the other hand, is small for these modes when the waves propagate along the axis and increases considerably as the wave propagation direction becomes perpendicular to the axis. One of the transverse modes propagating parallel to the axis has a negative γ'' value. The low temperature limit γ_0' and γ_0'' were calculated by a numerical integration procedure and were found to be equal.

They also studied the variation of the Grüneisen parameters with wave vectors for the acoustic and optic branches when the wave is propagated (i) parallel and (ii) perpendicular to the unique axis. Parallel to the unique axis, the optical branches were found to have γ' and γ'' values independent of wave length. Perpendicular to the unique axis, the γ' and γ'' values of the transverse optic branches vary rapidly with wave-length. γ'' decreases as the wave vector approaches the end of the Brillouin zone, while γ' increases. For optic branches γ'' is larger than the γ' values. The values of $\gamma'(n)$, $\gamma''(n)$, ($n = 2, 4, 6$) were obtained from the moments of the frequency distribution function. It is found that $\gamma'(n) = \gamma''(n)$ as one should expect because an ideal hcp lattice would be isotropic in its behaviour. The high temperature limit of the $\gamma - s$, namely, $\gamma'(0)$ and $\gamma''(0)$, were found by drawing a graph between $\gamma'(n)$ vs. n and finding the intersection with the axis $n = 0$. For different values of m and n , the limits of γ , namely $\gamma_\infty' = \gamma_\infty'' = \gamma(0)$ and $\gamma_0' = \gamma_0'' = \gamma(-3)$ were found. It was concluded that the variation with temperature of the effective Grüneisen functions should be only about 0.2 and the Grüneisen functions should

decrease as the temperature falls. A detailed calculation of the temperature variation of the Grüneisen function was made for the case $m + n = 9$. It was found that γ_T' was nearly equal to γ_T'' over the entire temperature range and the expected drop in γ_T' was found.

Ranji Rao & Srinivasan (886) have also indicated how the generalized Grüneisen parameters for the acoustic modes can be calculated for the third-order elastic constants. They have applied the method to calculate the Grüneisen parameters of the acoustic modes in alpha-quartz using the third-order elastic constants of McSkimin et al. (1530).

The generalised GPs for the elastic modes of calcite were calculated from the measured third-order elastic constants (Kaga 1433) by Ramachandran & Srinivasan (1632). These calculations reveal a large number of quasi-transverse elastic waves having negative values of γ' and γ'' . Unlike in the case of zinc, in calcite γ_0' is negative and γ_0'' is positive. The elastic compliance coefficients in calcite indicate that the Poisson contraction along the direction perpendicular to the unique axis due to the intrinsic thermal expansion parallel to the axis will be small. At low temperatures the negative expansion in calcite arises primarily because of the negative Grüneisen parameters of a large number of quasi-transverse elastic modes. Using the anisotropic continuum approximation it is shown that the negative expansion of calcite along the basal plane perpendicular to the unique axis at high temperature is probably due to the Poisson contraction arising from large positive expansion coefficient α_0 at these temperatures outweighing the small positive intrinsic expansion coefficient perpendicular to the axis.

Munn (1557) has recently indicated the role played by the linear compressibilities and the Grüneisen functions γ_T' and γ_T'' in determining the linear expansion coefficients α_0 and α_L of uniaxial materials. Equation (3.6.3) may be written as

$$V\alpha_0 = C_1 \{ \chi_0 \gamma_T' - 2S_{13}(\gamma_T'' - \gamma_T') \} \quad (3.6.5a)$$

$$V\alpha_L = C_1 \{ \chi_L \gamma_T' + S_{13}(\gamma_T'' - \gamma_T') \} \quad (3.6.5b)$$

where

$$\chi_L = S_{11} + S_{12} + S_{13} \quad (3.6.6)$$

$$\chi_0 = S_{33} + 2S_{13} \quad (3.6.6)$$

are the linear compressibilities perpendicular and parallel to the unique axis, respectively, and C_1 is the specific heat under constant stress. Now in a material in which the cross elastic modulus $S_{13} = 0$, (i.e., this would correspond to a layer lattice with negligible interaction among the layers) and the linear compressibilities are positive, the linear expansion co-

efficients follow faithfully the variations in γ'_T and γ''_T . In case there is no anisotropy in the Grüneisen functions, even if S_{13} is not zero, the cross term will vanish and the sign of the expansion would depend on the sign of the corresponding linear compressibility. For example, in arsenic, S_{13} is large and negative and χ_1 is negative. At low temperatures the Grüneisen functions γ'_T and γ''_T are nearly equal. This minimises the importance of the cross term involving S_{13} and α_1 is negative following the sign of χ_1 . As the temperature increases γ' becomes larger than γ'' and the cross-contribution becomes positive and overweigh the influence of negative compressibility. Hence the overall behaviour of the linear expansion coefficients of a uniaxial crystal could be quite complicated.

Srinivasan & Ramji Rao (1725, 1726) have used the Keating's (1437, 530) approach to work out the lattice dynamics, third-order elastic constants and thermal expansion of the hexagonal metals magnesium, zinc and beryllium. In this approach, the potential energy is written in powers of the changes in scalar products of interatomic vectors. Keating's approach has the advantage that the potential is automatically invariant towards rigid rotations. The application of the rotational invariance conditions leads to a large number of relations between the second and third-order coupling parameters which makes the coupling parameter approach very cumbersome to use. It is not claimed that Keating's approach is any more fundamental than the coupling parameter approach; its advantage lies in its ease of handling. Using two body and three body forces up to the fifth neighbours and anharmonic interactions to arise only from the two body forces, expressions were worked out for the coupling coefficients and the third-order elastic constants of hexagonal metals. Three anharmonic parameters in the two body interactions between the first, second and third neighbours are found to reproduce the pressure derivatives of the second-order elastic constants in magnesium and beryllium and the third-order elastic constants in zinc. The generalised GPs γ'_{ji} , γ''_{ji} have been calculated for the various normal modes and the temperature dependence of the effective Grüneisen functions γ'_T and γ''_T computed. In magnesium, the theoretical curve for γ'_T is in good agreement with the experimental measurements of McCammon & White (703) while γ''_T is about 10% higher than the experimental values. In zinc, the γ''_T vs. T curve exhibits a steep maximum at low temperatures. While the shapes of the theoretically calculated lattice Grüneisen functions γ'_T and γ''_T are similar to the experimentally observed variation of the total Grüneisen functions by McCammon & White (703) the theoretical curves are much higher than the experimental values. The reason for the discrepancy is the extreme sensitivity of the GPs of the low frequency modes corresponding to wave vectors lying at the vertical edge of the

Brillouin zone. The low temperature limit of γ''_T which can be determined from the experimental third-order elastic constant data of Swartz & Elbaum (1741) does not agree with the value obtained by Barron & Munni (71) from an analysis of the thermal expansion of zinc. Possibly the choice of the electronic Grüneisen parameters by Barron & Munni for zinc is not correct. In the case of beryllium there is no reliable thermal expansion data to compare with the calculations.

3.7. RIGOROUS THEORY OF THERMAL EXPANSION

A rigorous theory of thermal expansion of a crystal should start with the expression for the Helmholtz free energy which includes the contributions from cubic and quartic anharmonic terms in the potential energy

$$F = \Phi_0 + F_v^{(0)} + F_v^{(3)} + F_v^{(4)} \quad (3.7.1)$$

Here Φ_0 is the static energy of the crystal when the atoms are in their equilibrium positions, $F_v^{(0)}$ is the vibrational contribution to the free energy in the Harmonic approximation, $F_v^{(3)}$ and $F_v^{(4)}$ are the contributions to the free energy from the cubic and quartic anharmonic terms.

Starting with the Hamiltonian for the crystal

$$\begin{aligned} \mathcal{H} = & \frac{1}{2} \sum_{lk\alpha} M_k \cdot \dot{u}_k^2 \left(\begin{matrix} l \\ k \end{matrix} \right) + \frac{1}{2} \sum_{lk\alpha} \Phi_{ab} \left(\begin{matrix} l \\ k \end{matrix} \right) \cdot u_k \left(\begin{matrix} l \\ k \end{matrix} \right) \cdot u_k \left(\begin{matrix} l \\ k \end{matrix} \right) \\ & + \frac{1}{6} \sum_{lk\alpha} \Phi_{abc} \left(\begin{matrix} l \\ k \end{matrix} \right) \cdot u_k \left(\begin{matrix} l \\ k \end{matrix} \right) \cdot u_k \left(\begin{matrix} l \\ k \end{matrix} \right) \cdot u_k \left(\begin{matrix} l \\ k \end{matrix} \right) \\ & + \frac{1}{24} \sum_{lk\alpha} \Phi_{abcd} \left(\begin{matrix} l \\ k \end{matrix} \right) \cdot u_k \left(\begin{matrix} l \\ k \end{matrix} \right) \cdot u_k \left(\begin{matrix} l \\ k \end{matrix} \right) \cdot u_k \left(\begin{matrix} l \\ k \end{matrix} \right) \cdot u_k \left(\begin{matrix} l \\ k \end{matrix} \right) \end{aligned} \quad (3.7.2)$$

Maradudin et al. (679, 680) have obtained expressions for $F_v^{(0)}$, $F_v^{(3)}$ and $F_v^{(4)}$. In the above expression for the Hamiltonian, α is the component index, k the particle index, l the cell index, M_k is the mass of the k th particle, $u_k \left(\begin{matrix} l \\ k \end{matrix} \right)$ is the α component of the displacement of particle k in the cell

l , and

$$\Phi_{\alpha\beta\dots}\left(\begin{matrix} l' & \dots & l' \\ k & k' & \dots & k' \end{matrix}\right) = \dots \frac{\partial}{\partial u_{\beta}\left(\begin{matrix} l' \\ k' \end{matrix}\right)} \dots \frac{\partial}{\partial u_{\alpha}\left(\begin{matrix} l \\ k \end{matrix}\right)} \Phi \quad (3.7.3)$$

The above derivatives are evaluated at the equilibrium position $R_{\alpha}\left(\begin{smallmatrix} l \\ k \end{smallmatrix}\right)$ of the lattice. This position is different from the positions of the atoms $\bar{R}_{\alpha}\left(\begin{smallmatrix} l \\ k \end{smallmatrix}\right)$ obtained by minimising only the potential energy. The $R_{\alpha}\left(\begin{smallmatrix} l \\ k \end{smallmatrix}\right)$ are obtained by minimising the free energy. The expressions for $F_v^{(0)}$, $F_v^{(3)}$ and $F_v^{(4)}$ obtained by Maradudin et al. are given below:

$$F_v^{(0)} = \frac{1}{2} \hbar \sum_{\mathbf{q}j} \omega(\mathbf{q}j) + kT \sum_{\mathbf{q}j} \ln[1 - \exp(-\hbar \omega(\mathbf{q}j))] \quad (3.7.4)$$

$$F_v^{(3)} = -\frac{\hbar^2}{48N} \sum_{\mathbf{q}_1, \mathbf{q}_2, \mathbf{q}_3} \sum_{j_1, j_2, j_3} \Delta(\mathbf{q}_1 + \mathbf{q}_2 + \mathbf{q}_3) \frac{|\Phi(\mathbf{q}_1, j_1, \mathbf{q}_2, j_2, \mathbf{q}_3, j_3)|^2}{\omega(\mathbf{q}_1, j_1) \cdot \omega(\mathbf{q}_2, j_2) \cdot \omega(\mathbf{q}_3, j_3)} \cdot P(Q + U)$$

where

$$P = \prod_{s=1}^3 [1/(1 - \exp(-\hbar \omega(\mathbf{q}_s, j_s)))]$$

$$Q = \frac{1 - \exp\{-\hbar \omega(\mathbf{q}_1, j_1) + \omega(\mathbf{q}_2, j_2) + \omega(\mathbf{q}_3, j_3)\}}{\omega(\mathbf{q}_1, j_1) + \omega(\mathbf{q}_2, j_2) + \omega(\mathbf{q}_3, j_3)}$$

$$U = 3 \frac{\exp[-\hbar \omega(\mathbf{q}_3, j_3)] - \exp\{-\hbar[\omega(\mathbf{q}_1, j_1) + \omega(\mathbf{q}_2, j_2)]\}}{\omega(\mathbf{q}_1, j_1) + \omega(\mathbf{q}_2, j_2) - \omega(\mathbf{q}_3, j_3)}$$

$$F_v^{(4)} = \frac{\hbar^2}{32N} \sum_{\mathbf{q}_1, j_1, \mathbf{q}_2, j_2} \frac{\Phi(\mathbf{q}_1, j_1, \mathbf{q}_2, j_2, -\mathbf{q}_1, j_1, -\mathbf{q}_2, j_2)}{\omega(\mathbf{q}_1, j_1) \cdot \omega(\mathbf{q}_2, j_2)} \times \frac{\{1 + \exp[-\hbar \omega(\mathbf{q}_1, j_1)]\} \{1 + \exp[-\hbar \omega(\mathbf{q}_2, j_2)]\}}{\{1 - \exp[-\hbar \omega(\mathbf{q}_1, j_1)]\} \{1 - \exp[-\hbar \omega(\mathbf{q}_2, j_2)]\}} \quad (3.7.6)$$

Here $\omega(\mathbf{q}, j)$ are the lattice vibrational frequencies about the equilibrium position in the harmonic approximation. They are specified by a wave vector \mathbf{q} and a polarisation index j . N is the number of unit cells in the lattice. $\Delta(\mathbf{q}_1 + \mathbf{q}_2 + \mathbf{q}_3) = 1$, if $(\mathbf{q}_1 + \mathbf{q}_2 + \mathbf{q}_3)$ is a reciprocal lattice vector; it is zero otherwise. Its Fourier representation is

$$\Delta(\mathbf{q}_1 + \mathbf{q}_2 + \mathbf{q}_3) = \frac{1}{N} \sum_{\mathbf{l}} \exp 2\pi i(\mathbf{q}_1 + \mathbf{q}_2 + \mathbf{q}_3) \cdot \bar{\mathbf{R}}(\mathbf{l}) \quad (3.7.7)$$

$$\Phi(\mathbf{q}_1, j_1, \mathbf{q}_2, j_2, \dots, \mathbf{q}_j, j_j) = \sum_{\substack{l, k \\ l', k' \\ \vdots \\ l^{(s)}, k^{(s)}}} \frac{\Phi_{\alpha\beta\dots}\left(\begin{matrix} l & l' & \dots & l^{(s)} \\ k & k' & \dots & k^{(s)} \end{matrix}\right) \cdot \exp 2\pi i[\mathbf{q}_1 \cdot \bar{\mathbf{R}}(l') + \dots + \mathbf{q}_j \cdot \bar{\mathbf{R}}(l^{(s)})]}{[M_{\alpha} \cdot M_{\beta} \cdot \dots \cdot M_{\alpha^{(s)}}]^{1/2} \cdot \bar{\epsilon}_{\alpha}(k|\mathbf{q}_1, j_1) \cdot \bar{\epsilon}_{\beta}(k'|\mathbf{q}_2, j_2) \cdot \dots \cdot \bar{\epsilon}_{\alpha^{(s)}}(k^{(s)}|\mathbf{q}_j, j_j)}$$

The $\bar{\epsilon}(k|\mathbf{q}, j)$ are the eigenvectors for the different normal modes.

The free energy F can thus be evaluated as a function of the lattice parameter and temperature. By minimising the free energy with respect to the lattice parameters, one obtains the lattice constants as a function of temperature.

The central problem in the above procedure is, therefore, the calculation of $F_v^{(3)}$ and $F_v^{(4)}$. Maradudin et al. (679, 680) have attempted to solve this problem by (i) substituting the Fourier representation of $\Delta(k)$ and (ii) reducing the resulting summation over the \mathbf{q}_j s into products of sums over single wave vectors and polarisation index. This results in a considerable simplification of the computations involved. They have evaluated the resultant sums in a three-dimensional fcc lattice with nearest neighbour central interaction to obtain an expression for the free energy in powers of $\eta = 1/kT$ at high temperatures. Applying this model to lead, they calculated the thermal expansion of lead at high temperatures. They also evaluated the approximation used by Leibfried & Ludwig (634) who replaced $\omega^2(\mathbf{q})$ in the denominator of the expressions by the mean square frequency and found this approximation leads to a considerable simplification in the computation of $F_v^{(3)}$ without much loss in accuracy. Bicknese (97) has repeated the work of Maradudin et al. on fcc crystals with nearest neighbour central interaction. He has utilised a different approach in evaluating $F_v^{(4)}$. He has considered terms arising from fourth and third derivatives of the potential energy. The inclusion of the third derivatives of the potential energy, which was omitted by Maradudin et al. in the evaluation of $F_v^{(4)}$ is shown to change $F_v^{(4)}$ substantially. It appears that extensive numerical computation cannot be avoided in using the rigorous theory to calculate the thermal expansion at intermediate and high temperatures.

3.8 ANALYSIS OF THE SPECIFIC HEAT AND THERMAL EXPANSION DATA AT HIGH TEMPERATURES TO GET THE EXPLICIT ANHARMONIC CONTRIBUTIONS:

In the last section we saw that the free energy consists of contributions from the cubic and quartic interaction terms in the potential energy.

We may now write the vibrational contribution to the free energy as

$$F = F^{qh} + F^{anh} \quad (3.8.1)$$

where F^{qh} is the quasi-harmonic contribution and F^{anh} the anharmonic contribution. At high temperatures $T > \Theta$

$$\frac{F^{anh}(T, V)}{3Nk} = K - \frac{1}{2} A^* T - \frac{1}{3} B^* T^2 \quad (3.8.2)$$

We may divide the entropy and the specific heat also into quasi-harmonic and anharmonic contributions and obtain

$$\frac{S^{anh}(T, V)}{3Nk} = A^* T + B^* T^2 \quad (3.8.3)$$

$$\frac{C_V^{anh}(T, V)}{3Nk} = A^* T + 2B^* T^2 \quad (3.8.4)$$

where A^* and B^* are constants. We may define a Grüneisen parameter γ^{anh} for the anharmonic part of the entropy as

$$\gamma^{anh} = \frac{1}{C_V^{anh}} \frac{\partial S^{anh}}{\partial \ln V} \quad (3.8.5)$$

To a first approximation

$$\gamma^{anh} = \frac{\partial \ln A^*}{\partial \ln V} \quad (3.8.6)$$

The total Grüneisen function γ obtained from experiment is

$$\gamma = \frac{\gamma^{qh} C_V^{qh} + \gamma^{anh} C_V^{anh}}{C_V^{qh} + C_V^{anh}} \quad (3.8.7)$$

Here γ^{qh} is the quasi-harmonic Grüneisen parameter. The analysis of C_V^{qh} and γ^{qh} from specific heat and thermal expansion data at temperature $T < \Theta/2$ to obtain the moments μ_n and the Grüneisen function $\gamma(n)$ was described in section 3.2. It must be realised that even at low temperatures there is an explicit anharmonic contribution to the specific heat and thermal expansion and this is taken into account in a self-consistent way as follows:

(i) High temperature data are analysed roughly to get a first approximation to the anharmonic correction. Then some form of temperature dependence of these contributions is assumed and the anharmonic contribution so calculated is subtracted from the measured quantity to give a first estimate of the quasi-harmonic contribution. In the analysis of the

specific heat to find the even moments we convert the quasi-harmonic contributions to the specific heat into an equivalent Debye temperature $\Theta_D(V, T)$ and then correct $\Theta_D(V, T)$ to a constant volume making use of the relation

$$\frac{\Theta_D(V, T)}{\Theta_D(V_0, T)} = \left(\frac{V_0}{V} \right)^{\gamma(2)} \quad (3.8.8)$$

Then the analysis of $\Theta_D(V, T)$ is carried out as mentioned in section 3.2. To get the even moments of the frequency spectrum. Once the moments are found we evaluate the quasi-harmonic contribution to the specific heat at high temperature and subtract it from the measured C_V to obtain the explicit anharmonic contribution. This procedure is repeated to achieve self-consistency. This way C_V^{anh} is obtained. In the case of the Grüneisen function a similar procedure is adopted to get γ^{anh} , while C_V^{anh} is determined fairly precisely, the error in γ^{anh} is quite large. Leadbetter and coworkers (1491-1496) have measured the specific heat of lead, aluminium, NaCl, KCl, KBr and Ge at high temperatures. The data have been analysed to get the anharmonic constants A^* , B^* and γ^{anh} . Table 3.5 gives the values of these constants.

In the case of metals one should correct for the electron contribution to the specific heat and thermal expansion. At high temperatures theory predicts that the electronic contribution to the specific heat (C_{el}) will approach the contribution from free electrons, while at low temperatures C_{el} will differ from the free electron value. Also the electronic GP at high temperatures must approach the free electron value of $2/3$, while the effective GP at low temperatures has a different value. There is no experimental evidence to show whether these predictions are correct. So in the case of the metals Pb and Al in Table 3.5 the row a refers to the values of the anharmonic parameters evaluated after correcting for the electronic contribution to the specific heat and thermal expansion, using the free

TABLE 3.5 Anharmonic Parameters of Some Cubic Crystals

Material	A^* in $10^{-5}/^\circ K$	B^* in $10^{-9}/^\circ K^2$	γ^{anh}
Pb (a)	-10 \pm 3	6	8
(b)	-16 \pm 4	8	6
Al (a)	-1.9 \pm 0.9	—	-3 < γ^{anh} < 2
(b)	-3.5 \pm 1.5	—	—
Ge	3.1 \pm 1.0	1.4 \pm 1	4.5
NaCl	-1.5 \pm 0.9	positive	7 \pm 3
KCl	2.8 \pm 0.7	1.0	-5 \pm 2
KBr	3.5 \pm 1.0	1.4	-5 \pm 2

electron values of C_{cr} and γ_e , and row b refers to the values evaluated when the electronic contribution is obtained using the low temperature limits of C_{cr} and γ_e .

As far as the contribution to the parameter A^* is concerned, that from $F^{(4)}$ is negative and that from $F^{(3)}$ is positive. We see that in the metals lead and aluminium the quartic anharmonic contribution is more than the cubic anharmonic contribution. This is in general agreement with the calculations for a fcc crystal on the basis of simple models (Maradudin et al., 1980). In the case of germanium, which is an open structure, the cubic anharmonic contribution is more dominant than the quartic. Foreman (1950) made a calculation of A^* from phenomenological continuum model for germanium and his calculated value of A^* agrees well with experiment. In the case of the alkali halides the sign of A^* depends on the cation. In NaCl, quartic anharmonic term is dominant while in KCl and KBr the cubic anharmonic terms are dominant. Leibfried & Ludwig (1964) calculated the values of A^* on a rigid ion model for the three alkali halides mentioned above. While the sign of A^* is correct in all cases, the magnitude of A^* calculated was three to four times that found experimentally. Cowley & Cowley (1971) made similar calculations with the shell model for KBr; but their results show no significant improvement over the earlier calculations of Leibfried & Ludwig (1964). Cowley (1977) has calculated the anharmonic contribution for NaCl using a breathing shell model. The short-range polarisability of sodium was neglected and only nearest neighbour overlap interaction was assumed. The chlorine ion is taken to be breathing with the breathing force constant different from the core shell force constant. In addition to the quasi-harmonic approximation the contribution of the cubic and quartic terms to the free energy of the order T^2 were evaluated. The results showed that the contribution from the cubic and quartic anharmonic terms to the free energy are of the opposite sign and tend to cancel each other till 200°K. Below this temperature the quasi-harmonic approximation is good. Beyond 200°K ($T_M/4$, where T_M is the melting temperature of the solid) and up to $2T_M/3$ the inclusion of the first order anharmonic terms in the free energy gives good results.

It should also be mentioned here that for a few crystals the phonon frequencies have been measured as a function of temperature by inelastic neutron scattering. The total shift in the average frequency of the spectrum is due to (i) the change in volume of the crystal due to thermal expansion and (ii) the change in temperature.

$$\frac{\Delta\omega_D(0)}{\omega_D(0)} = -\gamma(0) \frac{\Delta V}{V} + \delta(0) \frac{\Delta E}{3Nk} \quad (3.8.9)$$

Here ΔE is the increase in energy of the crystal, $\gamma(0)$ is the average Grüneisen parameter for the crystal and $\delta(0) = -\partial \ln \omega_D(0)/\partial \ln T$. We can show that $\delta(0) \rightarrow -A^*$ and so one can calculate the fractional shift in the average frequency from the values of A^* given above and compare them with the measurements. It is noteworthy that in germanium the volume expansion coefficient is small due to the negative GPs of the transverse acoustic modes. Hence the pure temperature shift in the average frequency is quite large. This is not so with the other materials investigated. In every case the shift in the mean frequency calculated from the parameters obtained by an analysis of the thermodynamic data at high temperatures is in fair agreement with the observed results from inelastic neutron scattering.

3.9. NEGATIVE THERMAL EXPANSION IN SOLIDS

In systems like glasses and crystals having diamond like structure the negative value for α arises at low temperatures from the vibrational energy of the lattice. An explanation for the possible existence of negative α in these solids was proposed by Blackman (196, 107, 108) in a series of papers by adopting Barron's theoretical treatment. Using the relation

$$\gamma_i = \frac{d \ln (V^{-1/3} v_i)}{d \ln V} \quad (3.9.1)$$

Blackman arrived at the form

$$\gamma_i = -\frac{1}{6\rho v_i^2} \left[\frac{d(\rho v_i^2 r)}{dr} \right]_{r=r_0} \quad (3.9.2)$$

where v_i = velocity of propagation of the i th elastic mode ($i = 1, 2, 3$),

ρ = density,

$2r$ = lattice constant,

$c_{xi} = v_i^2 \rho$, is the elastic constant,

γ_i = Grüneisen parameter for the i th mode, and
 V = molar volume.

Two models were discussed by him. In the NaCl model, based on pure ionic interaction potential having Coulombic and repulsive forms, Blackman found that γ_i assumes negative values for transverse modes. Calculations for ZnS structure indicate that as long as the next nearest neighbour interactions are Coulombic, the transverse modes in the ZnS structure show negative values for γ_i for long range nearest-neighbour interactions.

Diamond-structure solids, for instance, are said to have a low-lying

transverse acoustic branch which at low temperatures is predominant in absorbing energy. In the case of glasses the presence of low-lying transverse optic modes, which are propagated with a lower velocity in comparison with longitudinal waves, is said to yield negative γ values at low temperatures. At these temperatures only acoustic vibrations are present, and the average value of γ can also become negative in which case the material possesses negative α . The large effect of the transverse modes in all these materials is due to open structure of these solids which result in large value of the shear elastic compliances associated with these modes. However, in NaCl, almost all the modes have positive γ .

On the other hand, anisotropic solids like FeF_2 , RuO_2 , CrO_2 exhibit negative values of α at high temperatures along one of the two principal directions. Therefore the explanation given above ceases to have any sense in these materials. This may be understood probably in the same way as in the case of rutile. In rutile Kirby (548) suggests that the thermal expansion arises from the contributions from the acoustic and optic modes such that optic modes are more effective in the c -direction whereas the acoustic modes are highly predominant along directions normal to the c -axis.

Negative values of α found in a few metals, for example, chromium, invar and gadolinium, arise from magnetic interaction or the electron gas (White 1147; Klein & Mountain 554). White has presented a simple picture to explain qualitatively the occurrence of negative values of α in crystals.

CHAPTER 4

Thermal Expansion and Phase Transitions

4.1. RELATION BETWEEN β , C_p AND χ_T NEAR A PHASE TRANSITION

It is well known that there exists in solids two kinds of phase transitions: the *first-order* (also known as first kind), and the *second-order* (variously referred to as continuous transitions, Curie points, lambda-points; transitions of higher order). The first-order transitions are characterized by discontinuous changes in energy, volume and crystal structure and by singularities in the first-order derivatives of the free energy. On the other hand, the second-order transitions are accompanied by continuous changes in energy and volume with singularities in the second-order derivatives of the free energy. Sometimes one distinguishes the onset of rotation of molecular groups within a relatively narrow temperature range as a third-order transition (or, homomorphous transition).

Gibb's phase theory is satisfactory for first-order transitions. Two phases can coexist over a range of pressure and temperature with their free energies \mathcal{G}_1 and \mathcal{G}_2 equal.

$$\left(\frac{\partial \mathcal{G}}{\partial T}\right)_P = -S$$

$$\left(\frac{\partial \mathcal{G}}{\partial P}\right)_T = -V \quad (4.1.1)$$

This leads to the famous *Clausius-Clapeyron relation*, namely,

$$\frac{dP}{dT} = \frac{L}{T(V_2 - V_1)} \quad (4.1.2)$$

where L is the latent heat involved in the transition, V_2 and V_1 are the volume of the crystal before and after the transition. Measurements of rates of transitions give some information about the free energy barriers separating the different modifications.

Ehrenfest (293) attempted to extend the Gibb's phase theory to include

the phase transition of the second-order. Accordingly, a transition is one of n th-order if it has a discontinuity in the n th derivative of the free energy. Therefore second-order derivatives like β , C_p and χ_T show discontinuities in a second-order phase transition. Abrupt changes in these thermodynamic quantities are related by Ehrenfest's equation. To derive this let us remind ourselves that the entropy and the volume are continuous at a second-order transition.

$$S_1 = S_2, \quad V_1 = V_2$$

$$\left. \frac{\partial S_1}{\partial T} \right)_P \cdot \delta T + \left. \frac{\partial S_1}{\partial P} \right)_T \cdot \delta P = \left. \frac{\partial S_2}{\partial T} \right)_P \cdot \delta T + \left. \frac{\partial S_2}{\partial P} \right)_T \cdot \delta P$$

$$\left. \frac{\partial V_1}{\partial T} \right)_P \cdot \delta T + \left. \frac{\partial V_1}{\partial P} \right)_T \cdot \delta P = \left. \frac{\partial V_2}{\partial T} \right)_P \cdot \delta T + \left. \frac{\partial V_2}{\partial P} \right)_T \cdot \delta P \quad (4.1.3)$$

Rearranging one gets

$$\frac{dP}{dT} = - \frac{\left. \frac{\partial S_2}{\partial T} \right)_P - \left. \frac{\partial S_1}{\partial T} \right)_P}{\left. \frac{\partial S_2}{\partial P} \right)_T - \left. \frac{\partial S_1}{\partial P} \right)_T} = - \frac{\left. \frac{\partial V_2}{\partial T} \right)_P - \left. \frac{\partial V_1}{\partial T} \right)_P}{\left. \frac{\partial V_2}{\partial P} \right)_T - \left. \frac{\partial V_1}{\partial P} \right)_T} \quad (4.1.4)$$

Using Maxwell's relations, we arrive at the Ehrenfest equation

$$\frac{dP}{dT} = \frac{1}{TV} \cdot \frac{C_{p2} - C_{p1}}{\beta_2 - \beta_1} = \frac{\beta_2 - \beta_1}{\chi_{T2} - \chi_{T1}} \quad (4.1.5)$$

where dP/dT is the slope of the equilibrium curve in the $P-T$ diagram. Putting $C_{p2} - C_{p1} = \Delta C_p$; $\beta_2 - \beta_1 = \Delta\beta$ and $\chi_{T2} - \chi_{T1} = \Delta\chi_T$,

$$\frac{dP}{dT} = \frac{1}{TV} \frac{\Delta C_p}{\Delta\beta} = \frac{\Delta\beta}{\Delta\chi_T} \quad (4.1.6)$$

Although Ehrenfest's relations hold good it cannot be used in practice because a perusal of the experimental data of these thermodynamic quantities around the transition temperature cannot yield definite values for the parameters $\Delta\beta$, ΔC_p and $\Delta\chi_T$. Some of the theories which confirm Ehrenfest's relations are based on either thermodynamics or statistical mechanics. Of these mention should be made of the theories of Landau, Pippard and the Ising model (Kadanoff et al., 521). According to Landau abrupt changes in the group symmetry elements of the crystallographic phase take place during a second-order transition (Landau, 1487) whereas the density and more generally the electron density distribution in the crystal differs only slightly on either side of the transition.

In a lambda-transition (λ -transition), both expressions, $\Delta\beta = \infty$ and $\Delta C_p = \infty$, lead to an indeterminate parameter dP/dT . Pippard (847) using a "cylindrical approximation" for the entropy and volume surfaces, arrived at the following relations among the second-order derivatives of \mathcal{F} ,

$$\left. \frac{\partial^2 S}{\partial P^2} \right)_T = f''; \quad \frac{\partial^2 S}{\partial T \cdot \partial P} = -C''$$

and

$$\left. \frac{\partial^2 S}{\partial T^2} \right)_P = C^2 f''$$

where

$$C = \frac{dP}{dT}_\lambda = - \frac{\left. \frac{\partial^2 S}{\partial T^2} \right)_P}{\left. \frac{\partial^2 S}{\partial T \cdot \partial P} \right)_P} \bigg/ \frac{\partial^2 S}{\partial T \cdot \partial P}$$

$$= - \frac{\left. \frac{\partial^2 S}{\partial T \cdot \partial P} \right)_P}{\left. \frac{\partial^2 S}{\partial T \cdot \partial P} \right)_P} \quad (4.1.7)$$

This leads to the Pippard's relations for the λ -transition,

$$C_p = CVT_\lambda \beta + \text{constant } (C_0) \quad (4.1.8a)$$

$$\beta = C \chi_T + \text{constant } (\beta_0) \quad (4.1.8b)$$

where

$$\beta_0 = \frac{C}{V} \frac{\partial V}{\partial P}_\lambda$$

and

$$C_0 = CT_\lambda \left. \frac{\partial S}{\partial P} \right)_\lambda$$

and T_λ refers to the λ -point.

$C_p - \beta$ relation due to Pippard was found to be true, quantitatively, in the case of ammonium chloride over the range 5°K below T_λ (242.8°K). In the case of dielectric and magnetic materials lambda-transitions have been treated using the Pippard relations (Wright 1811), and for ferroelectric transitions there is a recent report by Gibson & Wright (1371).

Interrelation between elastic modulus, specific heat and thermal expansion at a phase transition, which includes ferroelectric transitions, in crystals has been described recently by Testardi (1750).

4.2. EXPERIMENTAL DATA ON AMMONIUM COMPOUNDS

Most of the systematic investigations carried out on the variation of lattice constant with respect to temperature through phase transitions

in ammonium halides were by Hovi and his coworkers in Finland.
 NH_4Cl :

At present it is known that NH_4Cl has at least three modifications as follows:

Mod. I (NaCl structure) $\xrightarrow{456.1^\circ\text{K}}$ Mod. II (CsCl structure)

Mod. II (CsCl structure) $\xrightarrow{242.6^\circ\text{K}}$ Mod. III (CsCl structure)

The transition, mod. I \leftrightarrow mod. II, is characterized by the change of the coordination number from 8 to 6. The coordination number does not change at the other transition. The nature of the transition at 242.6°K has been studied dilatometrically by Adenstedt (4), Bridgman (137), Smits and MacGillavry (1016), and Thomas & Slaveley (1080). The transition is one of λ -type, and it is seen that for the range 237.5° to 242.6°K the $\beta - C_p$ plot is a straight line (Pippard, 847). Poyhonen (853) dilatometrically measured the total volume changes at the transition temperature of 456.1°K . He confirmed that the transition was one of first order. It has been shown indirectly that the volume changes discontinuously at 456.1°K . He obtained a change in volume Δv of $0.1315 \text{ cm}^3/\text{gm}$ (19.31%) at this transition. Arell (27) has determined the transition energy in NH_4Cl at 456.1°K as $L = 1073 \text{ Cal/mole}$ ($\pm 1.5\%$). From these data Poyhonen (853) obtained the value of dT_0/dp , from the Clausius-Clapeyron relation, as 0.0724°K/atm . The value of β in the modification II does not vary anomalously near the transition; and $\beta_1 < \beta_n$ near the transition. Therefore the value of β does not vary anomalously at the transition, thereby proving that the transition is one of first-order satisfying the Clausius-Clapeyron relation.

NH_4Br and ND_4Br :

In NH_4Br and ND_4Br the following modifications have been observed (for example, see Hovi, Paavola & Urvas (469)).

Mod. I (NaCl) $\xrightarrow{\text{NH}_4\text{Br at } 411^\circ\text{K}}$ Mod. II (CsCl)

Mod. II (CsCl) $\xrightarrow{\text{NH}_4\text{Br at } 235^\circ\text{K}}$ Mod. III (tetragonal)

Mod. III (Tetrag) $\xrightarrow{\text{NH}_4\text{Br at } 102^\circ\text{K}}$ Mod. IV (CsCl)

Investigations have been done recently by means of X-ray diffraction on the transitions at 411°K in NH_4Br (Poyhonen et al., 855; Hovi et al., 469) at 235°K (Hovi et al., 469, 473) in NH_4Br and the one at 102°K in

NH_4Br and 164°K in ND_4Br (Hovi et al., 469, 470), whereas Poyhonen (853) and Smits et al. (1015) reported dilatometric measurements of the transitions I-II and II-III of NH_4Br and ND_4Br . Also, the III-IV transition in ND_4Br has been studied dilatometrically by Smits et al. (1015).

As in the case of NH_4Cl , Poyhonen (853) used the data $L = 882 \text{ cal/mole}$ ($\pm 3\%$) of Arell (27) and $\Delta V = 0.0795 \text{ cm}^3/\text{gm}$ (18.85%) for NH_4Br at 411°K I-II transition. He observed the transition to be a first order with the Clausius-Clapeyron relation holding good. The pressure derivative dT/dp was calculated to be 0.0878°K per atm. In the case of NH_4Br I-II transition, the value of β does not show any discontinuous change. It is clearly seen from the study of Hovi et al. (469), Poyhonen et al. (855) and Hovi et al. (470) that in both NH_4Br and ND_4Br , the volume changes discontinuously at all the three transition temperatures. The data reported by them are:

NH_4Br II-I $\Delta V = 7.54 \text{ cm}^3/\text{mole}$ (18.3%)

ND_4Br II-I $\Delta V = 7.61 \text{ cm}^3/\text{mole}$ (18.5%)

NH_4Br III-II $\Delta V = -0.173 \text{ cm}^3/\text{mole}$ (-0.43%)

ND_4Br III-II $\Delta V = -0.293 \text{ cm}^3/\text{mole}$ (-0.73%)

NH_4Br IV-III $\Delta V = 0.854 \text{ cm}^3/\text{mole}$ (2.20%)

ND_4Br IV-III $\Delta V = 0.873 \text{ cm}^3/\text{mole}$ (2.23%)

The temperature dependence of the molar volumes of NH_4Br and ND_4Br has been expressed by polynomial equations, for all the four modifications by Hovi et al. (469). No calculations on the dT/dp have been performed so far in these transitions other than II-I in NH_4Br .

NH_4I and ND_4I :

NH_4I and ND_4I are known to possess three modifications as follows:

Mod. I (NaCl) $\xrightarrow{\text{NH}_4\text{I at } 257^\circ\text{K}}$ Mod. II (CsCl)

Mod. II (CsCl) $\xrightarrow{\text{NH}_4\text{I at } 224^\circ\text{K}}$ Mod. III (tetragonal)

Hovi & Varteva (473) and Hovi & Lainio (466) have studied by means of X-rays the transitions I-II and II-III, respectively, in NH_4I . Very recently, Hovi et al. (468) have studied the unit cell dimensions variation with temperature through the phase transitions I-II and II-III in both NH_4I and ND_4I .

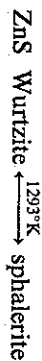
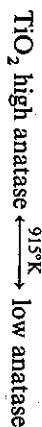
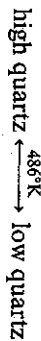
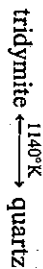
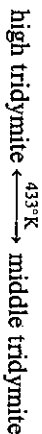
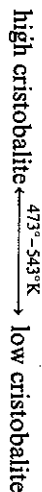
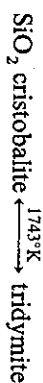
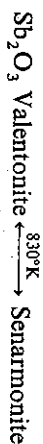
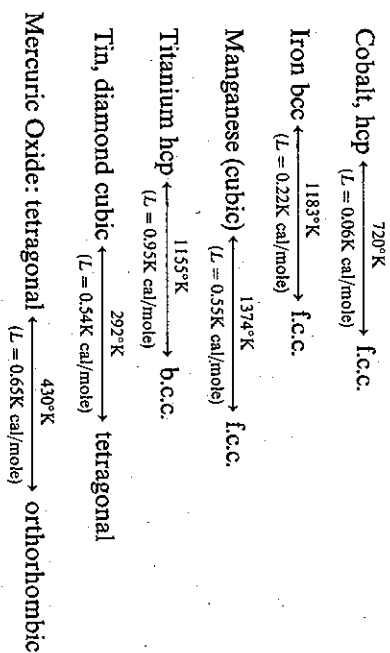
NH₄NO₃:

NH₄NO₃ is known to have two phase transitions, one at 357.1°K and the other at 398.8°K. Hovl, Poyhonen & Paalassalo (471) determined the dilatation of NH₄NO₃ through these transitions using a dilatometer. It is seen from their study that the specific volume changes discontinuously at these two temperatures. A total volume change of -0.00920 cm³/gm at 357.1°K was found as the temperature was increased. An increase of 0.0136 cm³/gm in the total volume is observed when the material undergoes a phase change at 393.8°K to high temperature modification. The highest modification has the maximum cubic thermal expansion coefficient. No other calculations are available on the properties at the transition temperatures.

RbNO₃:

Poyhonen et al. (857) measured the volume change to be +0.90 cm³/mole (1.82%) for RbNO₃ when it changes its low temperature phase to high temperature modification (III-IV) at 435°K, with a discontinuous change in volume. Using $L = 923 \text{ Cal/mole}$ of Arell & Varteva (28), dT/dP is reported to have been calculated by the authors. In addition to this, there are two more phase changes occurring in RbNO₃, viz., one at 492°K (II-III) and the other at a still higher temperature (I-II). But no study of thermal dilatation was performed at these phase transitions.

The following compounds are also found to exhibit phase transitions at various temperatures as indicated below, and no details of thermodynamic properties are available for these materials at the transition temperatures.

**4.3. THERMAL EXPANSION AND FERROELECTRICITY**

Certain classes of crystals are known to possess phase transitions below which they exhibit ferro-electric properties. Many crystals exhibiting such properties have been discovered in recent years (262, 508). The ferroelectric crystals so far developed are broadly classified under two types, namely, *displacive* or *hard* type and *soft* type. Crystals coming under the former type possess high dielectric constants and belong to the perovskite type of structures. BaTiO₃ is a typical crystal belonging to this type. The crystals coming under the latter type are usually hydrogen bonded. Rochelle salt is a typical crystal of this type. Any kind of phase transition in a crystal should give rise to anomalous behaviour in thermal expansion. It is well known that the anisotropy of the inter-molecular forces leads to anisotropy in thermal expansion of the crystal. The greatest change in the length of a hydrogen bonded crystal with temperature is in the direction of the weakest bonds, i.e., parallel to the directions of the hydrogen bonds. A study of the thermal behaviour of ferro-electric crystals is of very great importance for getting an insight into the nature of the phase transition.

In the case of a so-called *soft* ferroelectric containing hydrogen bonds, it is known that the hydrogen bonds are responsible for the orderly arrangement of atomic (or, molecular) electric dipole moments in the crystal. The crystal is then said to possess a spontaneous electric polar-

zation. In general ferro-electric crystals possess higher dielectric constants at ordinary temperatures, in particular, in the region of the Curie point. The applicability of Pippard's relations to ferro-electrics is reported elsewhere (1123).

Considering the dielectric constant, ϵ ,

$$\frac{\epsilon'}{\epsilon_0} - 1 = \frac{N}{V} \bar{\mu} \quad (4.3.1)$$

where $\bar{\mu}$ is the average molecular dipole moment per unit electric field, N is the number of molecular dipoles and V is the volume. Differentiation of this expression with respect to temperature, we get

$$\frac{d(\epsilon'/\epsilon_0)}{dT} = \left(\frac{\epsilon'}{\epsilon_0} - 1 \right) \left[\frac{1}{\bar{\mu}} \frac{d\bar{\mu}}{dT} - \beta \right] \quad (4.3.2)$$

This is evidently a relation between the temperature variation of dielectric constant and the coefficient of thermal dilatation and also the temperature coefficient of dipole moment. For a ferroelectric crystal (4.3.2) can be expressed in the form,

$$\frac{dP_s}{dT} = F \cdot P_s \quad (4.3.3)$$

where

$$F = \left[\frac{1}{\epsilon} \frac{d\epsilon}{dT} + \beta \right] + F_0$$

assuming that $\bar{\mu} \propto P_s$, P_s is the spontaneous polarisation of the ferro-electric. Thus there is an intimate connection between thermal expansion and spontaneous polarization through anharmonicity in the potential energy of the crystal. And all ferro-electric crystals are characterized by the property of reversible spontaneous polarization, by external means below the Curie temperature T_c . In the case of H-bonded ferro-electrics, the mechanism of phase transition at T_c is attributed to the collapse of the non-linear H-bond force triggered by thermal expansion (486).

Ubbelohde & Woodward (1098) have shown that thermal expansion is largest in the direction of hydrogen bonds in Rochelle Salt, and this predominance largely disappears above the upper Curie point. (Rochelle salt crystal has two Curie points. A third phase transition at 212°K has been reported recently in JETP Lett. 19, 293 (1974)). Stretching of the short hydrogen bonds is supposed to cause the onset of dielectric anomalies at the lower Curie point and the resulting change of the non-polar structure of the crystal to a polar one. Study of the KH_2PO_4 -type crystals (38, 201, 877, 1453) reveals that the magnitude of the thermal expansion anomalies

at the transition point is markedly affected by deuteration. The anomalies observed in the ferro-electric alkali compounds are found to be smaller by one order of magnitude than those for the ammonium compounds. The shortest hydrogen bonds in the unit cell of triglycine sulphate are reported to be in a direction having the maximum value of thermal expansion (368). This is also found to hold good partly in the case of ferro-electric sodium trihydroseleinite (257, 260, 588). A mechanism for the thermal expansion in KNO_3 crystals has been proposed (10) on the basis of its structure being a packing of sheets of $\text{NO}_3\text{-K-NO}_3$. Measurements of the thermal expansion coefficients of many other ferro-electric crystals have been reported. These crystals are BaTiO_3 (507, 714, 944), GASH (304), sodium nitrite (9, 457, 689), copper formate (963), lead meta-niobate (400), strontium titanate (261, 662, 663), lithium tantalate (490), lithium hydrazinium sulphate (258), ferro-electric alums (257, 259), barium sodium niobate (1187), TGS (368, 986, 305, 1075, 1681, 1109, 1781), lithium niobate (1501), etc.

The thermal behaviour of a ferro-electric crystal is very much complicated as a result of the spontaneous lattice strain. It is a well known fact that the effect of an electric field on a piezoelectric crystal (all ferro-electric crystals are piezoelectrics) produces in addition to the electrostrictive strain (strain proportional to square of the field), the piezoelectric strain (strain proportional to the field). Denoting the piezoelectric strain constant by b , and the electrostrictive coefficient by Q , for a crystal free from mechanical stresses there exists a non-linear relation between strain x and polarization P (154). It is given by

$$x = bP + QP^2 \quad (4.3.4)$$

This holds good also in the polar region of the crystal (when $P = P_s$). The linear term, bP , will be zero for centrosymmetric phases of the crystal (example: BaTiO_3 above its T_c). Two important types of crystals exist according as whether the crystal is piezoelectric or not above T_c . BaTiO_3 and KH_2PO_4 are illustrative of the two types. One can, therefore, isolate the two contributions to thermal expansion, viz., thermal expansion due to induced strain and that due to spontaneous strain (piezoelectric strain resulting from the presence of P_s), as, for example, in LiTaO_3 (490).*

Instability of normal modes of vibration may arise from negative thermal expansion or anomalous positive thermal expansion in solids (29). If this is so, one can then link the above idea to explain the instability of certain transverse optic modes at the Curie point (154). The anomalous component of the thermal expansion near broad ferro-electric transitions has been analysed (912). The sign of the thermal expansion coefficient is governed by the sign of the volume electrostriction.

* (Note added in proof). The spontaneous strains have been isolated in Rochelle Salt by Imai K. (*J. Phys. Soc. Jap.*, 41, 2005-10 (1976)).

An analysis of the available data on the electrical properties of some ferro-electric crystals and their thermal expansion anisotropy through the Curie points has been reported (257). The crystals studied are barium titanate, lithium tantalate, lead meta-niobate, lead meta-tantalate, potassium dihydrogen phosphate, triglycine sulphate, sodium trihydro-selenite and sodium nitrite. The data on thermal expansion of isomorphous crystals should have been included in order to complete the discussion, since it is known that a representative crystal and its isomorphous compounds will have similar thermal behaviour. The unique direction along which the ferro-electric crystal has a predominant *negative anomaly* in thermal expansion in the region of the Curie point is found to coincide invariably with the direction of *maximum dielectric anomaly* (257, 589). The only crystal which does not obey the above rule is sodium nitrite. In a ferroelectric crystal the polar axis will have the same direction as that of the maximum dielectric anomaly in the crystal. These observations have been reported to hold good for crystals belonging to different ferro-electric classification, and irrespective of the nature of both the ferroelectric phase transition and symmetry of the phases between which the transition occurs. These are illustrated clearly in the case of sodium trihydro-selenite in Fig. 2.17 and Fig. 2.18. The polar axis of this crystal is along the [313] direction which is close to the axis (indicated by a) along which the dielectric anomaly is found to be predominant. Thermal behaviour of this crystal (257, 260, 588) reveals that there is negative thermal expansion along the α -axis. Since the unit cell dimensions of this crystal below T_c show that the symmetry of the ferroelectric phase deviates only very slightly from the symmetry of the paraelectric phase, it is but proper to assume that there may not be any change in the positions of the principal axes of the expansion ellipsoids on either side of the Curie point (-79°C). This leads to the positive conclusion that the polar axis in this crystal may be along the α -axis as revealed by the studies on thermal expansion. The ferroelectric [313] direction reported for this crystal is roughly along the α -axis as mentioned before.

Thus thermal expansion measurements made continuously and precisely in a temperature range can not only reveal the nature of phase change in a crystal in that range of temperature but also predict the direction of maximum dielectric anomaly in a ferroelectric crystal, and hence identify the possible orientation of the ferroelectric axis. This important observation leads to the conclusion that *any ferroelectric phase transition does involve a negative anomaly* in thermal expansion in a specified direction in the crystal (257, 589). Such measurements in a crystalline dielectric may even reveal if the crystal is a ferroelectric or anti-ferroelectric.

CHAPTER 5

Thermal Expansion Data

In the past two decades there has been an enormous growth of research activity in the field of methods of measurement of thermal expansion coefficients of crystals, as seen in Chapter 2. As in so many other branches of science, the active research worker is inundated by the *information explosion*. It is needless to emphasize the importance of readily accessible thermal expansion data for him. Tables containing thermal expansion data of substances studied till 1956 have been already published by Srinivasan & Krishnan (1041).

In this Chapter, a compilation of experimental data obtained from the literature up to 1975 is reported in the form of five Tables. Table 5.1, incorporates information at high temperatures for an exhaustive list of about 370 substances. On the other hand, Table 5.2, includes thermal expansion at very low temperatures (below $\Theta_D/20$) for about 48 crystalline solids. These two Tables facilitate also intercomparison of data measured by various research groups on a particular substance.

The linear thermal expansion coefficient, α , at temperature T expressed in $^\circ\text{K}$, can be calculated from an empirical equation of the form already discussed in Chapter 2. Accordingly,

(i) at high temperatures the empirical equation for a range of temperatures is given by

$$\alpha_T = A + B(T - T_0) + C(T - T_0)^2 \quad (5.1)$$

(ii) at very low temperatures the value of α can be obtained from (3.4.7.) and (3.5.3.) in the general form

$$\alpha_T = BT + DT^3 + ET^5 + \dots \quad (5.2)$$

where the various factors have the following significance:

- A is the linear thermal expansion coefficient at temperature $T_0(^\circ\text{K})$, i.e., α_{T_0} , and it is a factor expressed in $10^{-6}/^\circ\text{K}$,
- B denotes the factor, expressed in $10^{-9}/^\circ\text{K}^2$,
- C denotes the factor, expressed in $10^{-11}/^\circ\text{K}^3$,

- D denotes the factor, expressed in $10^{-11}/^{\circ}\text{K}^4$,
 E denotes the factor, expressed in $10^{-13}/^{\circ}\text{K}^6$, and
 T is the temperature in $^{\circ}\text{K}$.

The equations (5.1) and (5.2) are purely empirical in the sense that their forms are inferred from the results of experiment or observations and in which the "constants" A, B, C, D & E are determined from experimental or observational data. (The factor B in equations (5.1) and (5.2) does not have the same meaning.) In Table 5.1, and Table 5.2, these constants reported are from appropriate references indicated in the last column. In the case of substances for which no such constants are reported in the literature, the present authors have computed by means of a Least Squares procedure the best representative curve fitting the equation. Such cases are indicated by the symbol * in the remarks column 11 of the Tables. Another symbol @, in column 11 denotes that the constants A, B, etc., have been obtained by the present authors from equations of the type (2.2.12) or (2.2.13) in the literature. In column 8, the range of temperature for which the equation (5.1) or (5.2) is valid is given. Column 4 gives the value of T_0 ; but if no value is given then the lower limit of temperature in the range should be assumed for T_0 .

The numerical values of these quantities, A, B, etc., are given to two or three significant figures after the decimal point, which is sufficiently precise for most theoretical work or technical calculations. The number of figures after the decimal point varies in these tables. This is due to the circumstance that some solids have been studied precisely whereas others are not. Further, the accuracy of the results, wherever available, and the technique of measurement of α have been furnished in columns 9 and 10, respectively. The following abbreviations have been used to indicate the methods of measurement:

- X.R. : X-ray
 P : Pyrometer
 O.L. : Optic Lever
 2T-C : Two-terminal Capacitance
 3T-C : Three-terminal Capacitance
 V.T. : Variable Transformer
 G : Grid of Andres
 I : Interferometer
 Q.D. : Quartz Dilatometer
 H.D. : Henning's Dilatometer
 U : Ultrasonic
 and
 P.R. : Push-rod method

No effort has been made in classifying the different compounds reported in these tables. However, most of the compounds are arranged according to the crystal systems to which they belong (indicated by column 2).

In the case of anisotropic crystals, the direction of measurement in the crystal is indicated in column 3, with a , b , c , for the crystallographic a -, b -, c -axes, respectively, and 1, 2, 3, indicating the subscripts of the principal expansion coefficients. φ is the angle between one of the principal expansion coefficients with a crystal axis in the (010) plane.

There are solids for which the α -data at different temperatures are not systematically reported in the literature. For these solids the value of α only at a particular temperature is given in these tables.

In Table 5.3 the coefficients of thermal expansion of a few halides at different temperatures below 100°K are reproduced, instead of supplying the data in the form of empirical relations.

Accurate measurements of thermal expansions have been made recently on high-purity copper, silver, gold and potassium metals. Table 5.4 has been prepared on these metals. Study of inert gas solids has been of extensive use as model substances for calculations of thermodynamic properties based on lattice dynamics. It is, therefore, considered useful to reproduce recent thermal expansion data measured accurately on argon, krypton, xenon and neon in Table 5.5.

TABLE 5.1. Coefficients of Thermal Expansion at High Temperatures for Different Crystals
 $\alpha_T = A + B(T - T_0) + C(T - T_0)^2$

Substance 1	Crystal system 2	Axis 3	T_0 , °K 4	A ($10^{-6}/^\circ\text{K}$) 5	B ($10^{-9}/^\circ\text{K}^2$) 6
CUBIC ELEMENTS					
(1) Aluminium (Al)	Cubic			10.1 9.53 8.17 4.79 3.45 2.18 1.10 0.62	
(2) Argon (Ar)	"		257 1950		
(3) Cerium (Ce)	"		273	7.22	-9.55
(4) Caesium (Cs)	Cubic		285		
(5) Copper (Cu)	Cubic		273 70	16.872 8.648 9.72	1.773 69.95
(6) Diamond (C)	"		273	0.87 -0.2 ~ 0.3	9.228
(7) Germanium (Ge)	Cubic		273	6.05 -0.064 5.722	3.60
(8) Gold (Au)	Cubic		273 273 70	13.99 13.624 11.39	4.91 8.814 16.93
(9) Iridium (Ir)	Cubic		273	6.13 7.5 6.473	2.56 1.438
(10) Iron (α) (Fe)	Cubic		273 273 273	11.45 13.06 2.60	14.0 5.989
(11) Iron (γ) (Fe)	Cubic			19.54	0
(12) Krypton (Kr)	Cubic		193 430		

Range of temperature ($10^{-11}/^\circ\text{K}^3$) 7	Accuracy in % 9	Method 10	Remarks 11	Reference 12
at 90.6 at 80.7 at 70.2 at 58.8 at 49.6 at 39.5 at 30.2 at 25.2	5 5 5 5 5 5 5 5	I I I I I I I I		(357) " " " " " " "
at 25 at 81	10	Q.D.	Solid	(674) (1012)
323-973 at 301.4	3	I	" * Melting point = 301.4°K	(73) (1225)
323-623 90-330 at 93.3	5	Q.D. Q.D. I	* *	(636) (636) (357)
273-828 < 90	1	XR		(584) (783)
293-1085 at 30		XR V.T. XR		(997) (1024) (1241)
298-314 298-1151 323-623 90-330		XR XR Q.D. Q.D.	see also (357) * *	(285) (636) (636)
303-1138 at 445 303-2494		XR XR P.R.		(997) (279) (1393)
272-970 270-1181 at 69.9	5	XR I	except 988-1098°K	(487) (402) (357)
> 1170 at 25 at 100	10	XR Q.D.	Solid "	(402) (674) (658)

TABLE 5.5. (Contd.)
(ref. 1414) (3T-C)

Neon			
T(K)	$\beta(10^{-6}K^{-1})$	T(K)	$\beta(10^{-6}K^{-1})$
0.5	0.1005	9.0	782.4
1.0	0.8069	9.5	899.3
1.5	2.734	10.0	1020
2.0	6.537	11.0	1269
2.5	13.02	12.0	1542
3.0	23.19	13.0	1817
3.5	38.35	14.0	2108
4.0	59.97	15.0	2409
4.5	89.55	16.0	2700
5.0	128.3	17.0	2997
5.5	177.3	18.0	3312
6.0	236.4	19.0	3654
6.5	305.4	20.0	4011
7.0	383.8	21.0	4386
7.5	471.1	22.0	4764
8.0	567.0	23.0	5154
8.5	671.0		

Appendix I

(Note added in Proof)

Mode Grüneisen parameters, Pressure dependence of TA and LA phonons, and Inelastic scattering of neutrons in RbI and KBr.

There are classes of solids of certain structure and bonding types where for some phonon branches, Grüneisen parameters may be negative. Alkali halides are examples of this behaviour.

Studies on rubidium iodide by means of inelastic scattering of neutrons by Blaschko et al. (1243) yielded 43 values for the microscopic Grüneisen parameters accurate to within 2 to 10% in a few symmetry directions in the crystal. Their calculations of mode Grüneisen parameters based on breathing Shell Model predict both positive and negative signs for Grüneisen parameters for different phonon branches. In the different regions of the Brillouin zone, the observed values are consistent with the calculated mode Grüneisen parameters, showing the success of the theoretical model in the entire zone.

In potassium bromide measurements of microscopic Grüneisen parameters based on inelastic scattering of neutrons have been made recently by Blaschko et al. (Blaschko, O., Ernst, G. & Quitner G., *J. Phys. Chem. Solids*, **36**, 41-44 (1975)). Though a total of about 20 phonons, including TA and LA phonons, has been measured, only 7 phonons have been evaluated by these authors. Further they have measured pressure induced phonon frequency shifts in KBr using neutron scattering. The phonon peak intensities do not change with pressure in the LA branch, whereas peak intensities do change for TA phonons under the influence of pressure on the sample. The peak intensity increased for phonons having negative value for the Grüneisen parameters and the vice versa. Blaschko et al. have compared their results with several theoretical predictions, referred to in Section 3.5d(i) of the present volume, viz. shell model calculations by Cowley & Cowley (211), and by Ruppin & Roberts (1659), and the rigid iron model, simple deformation dipole model and advanced deformation dipole model calculations by Karo R.J., & Hardy A.M. (*Phys. Rev. B*, **7**, 4696 (1973)). The values of Grüneisen

parameters obtained from calculations differ considerably, especially in the TA (110) branch. Despite their differences all the theories agree at least qualitatively in predicting that negative Grüneisen parameters should be found throughout the TA (110) and TA (001) branches and the large-q part of the LA (110) branch, whereas in other branches the Grüneisen parameters are positive. These predictions are confirmed by the results of Blaschko et al. (*loc. cit.*). Further measurements of pressure induced frequency shifts on other simple crystals using inelastic neutron scattering technique are expected to throw more light on lattice models and crystal potential.

References

1. Abbe, *Wied. Ann.*, **38**, 453 (1889).
2. Abbiss C.P., Huzan E. and Jones G.O., *Proc. Seventh Intl. Conf. Low Temp. Phys. (Toronto)* 1960 (Univ. Toronto Press Ont.), pp. 688 (1961). Thermal Expansion of aluminum at low temperatures.
3. Abeledo de M.J., De Benyacat M.R. and Callori E.E., *Bol. Acad. Nac. Cienc. (Argentina)*, **42**, 241-3 (1961). Crystallographic study of potassium bromostannate (Spanish).
4. Adenstedt H., *Ann. Phys. (Leipzig)*, **26**, 69-96 (1936). Studien Zur thermischen Ausdehnung fester Stoffe in tiefer temperature (Cu, Ni, Zink Blende, LiF, Kalkspat, Aragonit, NH_4Cl) (German).
5. Alefeld B., *Z. Phys.*, **222**, 155-64 (1969). The change of lattice parameters of SrTiO_3 near the phase transition point at 108°K.
6. Aliev I.Yu., Lazarev B.G. and Sudorov A.I., *Sov. Phys.-JETP.*, **20**, 1358-61 (1965). Exptal. determination of the electronic part of the thermal expansion coefficient of Iron.
7. Amonenko V.M., Vyugov P.N. and Gumenyuk V.S., *High Temp.*, **2**, 22-4 (1964). Thermal Expansion of W, Mo, La, Nb and Zr at high temperatures.
8. Amoros J.L., Canut M.L. and Neira E., *Proc. Roy. Soc. London*, **A285**, 370-81 (1965). Thermal Expansion of β -succinic acid and α -adipic acid in relation to their crystal structures.
9. Amoros J.L., Gutierrez M. and Canut M.L., *Bol. R. Soc. Espan. Hist. Nat. (Geol.)*, **62**, 5-21 (1964). Sobre la dilatacion termica del nitrato sodico ferroelectrico NaNO_2 (Spanish).
10. Amoros J.L., Gutierrez M. and Canut M.L., *Bol. R. Soc. Espan. Hist. Nat. (Geol.)*, **62**, 23-39 (1964). La dilatacion termica del nitrato NO_3K (sal de piedra) (Spanish).
11. Anderson O.L., "Semiconductor Physics" *Conf. (Prague)*, pp. 649 (1960). A low temperature anomaly in silicon.
12. Anderson W.G., *Rev. Sci. Instrum.*, **39**, 1064-5 (1968). Filament dilatometer.
13. Andreeva T.V., Barantseva I.G., Dudnik E.M. and Yupko V.L., *High Temp.*, **2**, 742-4 (1964). Some Physical Properties of AlN.
14. Andres K., *Cryogenics*, **2**, 93-7 (1961). The measurement of thermal expansion of metals at low temperatures.
15. Andres K., *Proc. Eighth Intl. Conf. Low Temp. Phys. (London)*, 1962 pp. 397-8 (Butterworths, London) (1963). The thermal expansion of some metals at low temperatures.
16. Andres K., *Phys. Lett.*, **7**, 315-16 (1963). The thermal expansion of Molybdenum, Tungsten, Rhenium, Pt and Cd at low temperatures.